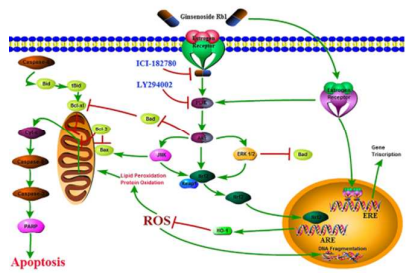




Ginsenoside Rb1 Prevents Hypoxia–Reoxygenation-Induced Apoptosis in H9c2 Cardiomyocytes via an Estrogen Receptor-Dependent Crosstalk among the Akt, JNK, and ERK 1/2 Pathways Using a Label-Free Quantitative Proteomics Analysis

Journal:	<i>RSC Advances</i>
Manuscript ID:	RA-ART-02-2015-002432.R1
Article Type:	Paper
Date Submitted by the Author:	05-Mar-2015
Complete List of Authors:	<p>Ai, Qidi; Institute of Medicinal Plant Development, Chinese Academy of Medical Sciences & Peking Union Medical College, Key Laboratory of Bioactive Substances and Resources Utilization of Chinese Herbal Medicine, Ministry of Education</p> <p>Sun, Guibo; Institute of Medicinal Plant Development, Chinese Academy of Medical Sciences & Peking Union Medical College, Key Laboratory of Bioactive Substances and Resources Utilization of Chinese Herbal Medicine, Ministry of Education</p> <p>Luo, Yun; Institute of Medicinal Plant Development, Chinese Academy of Medical Sciences & Peking Union Medical College, Key Laboratory of Bioactive Substances and Resources Utilization of Chinese Herbal Medicine, Ministry of Education</p> <p>Dong, Xi; Wenzhou Medical College, Academy of Chinese Materia Medica</p> <p>Hu, Ruifeng; Institute of Medicinal Plant Development, Chinese Academy of Medical Sciences & Peking Union Medical College, Key Laboratory of Bioactive Substances and Resources Utilization of Chinese Herbal Medicine, Ministry of Education</p> <p>Meng, Xiangbao; Institute of Medicinal Plant Development, Chinese Academy of Medical Sciences & Peking Union Medical College, Key Laboratory of Bioactive Substances and Resources Utilization of Chinese Herbal Medicine, Ministry of Education</p> <p>Sun, Xiaobo; Institute of Medicinal Plant Development, Chinese Academy of Medical Sciences & Peking Union Medical College, Key Laboratory of Bioactive Substances and Resources Utilization of Chinese Herbal Medicine, Ministry of Education</p>



Rb1 prevent H/R-induced apoptosis of H9c2 cells via an estrogen receptor-dependent crosstalk among the Akt, JNK, and ERK 1/2 pathways.

**Ginsenoside Rb1 Prevents Hypoxia–Reoxygenation-Induced
Apoptosis in H9c2 Cardiomyocytes via an Estrogen
Receptor-Dependent Crosstalk among the Akt, JNK, and ERK 1/2
Pathways Using a Label-Free Quantitative Proteomics Analysis**

Qidi Ai ^a, Guibo Sun ^{a,*}, Yun Luo ^a, Xi Dong ^b, Ruifeng Hu ^a, Xiangbao Meng ^a, and Xiaobo Sun ^{a,*}

^a Key Laboratory of Bioactive Substances and Resources Utilization of Chinese Herbal Medicine, Ministry of Education, Institute of Medicinal Plant Development, Chinese Academy of Medical Sciences & Peking Union Medical College, Beijing, 100193, P. R. China

^b Academy of Chinese Materia Medica, Wenzhou Medical College, Wenzhou, 325035, P.R. China.

* Corresponding author: Xiao-bo Sun, Gui-bo Sun, Institute of Medicinal Plant Development (IMPLAD), Chinese Academy of Medical Sciences and Peking Union Medical College, No. 151, Malianwa North Road, Haidian District, Beijing, 100193, P.R. China. Tel: +86-10-57833013. Fax: +86-10-57833013
E-mail: sun_xiaobo163@163.com (X.-b. Sun), sunguibo@126.com (G.-b. Sun)

Abstract

Reperfusion therapy is widely used to treat acute myocardial infarction (AMI). However, further injury to the heart that is induced by rapidly initiating reperfusion is often encountered in clinical practice. Ginsenoside Rb1 (Rb1) is the major active ingredient in processed *Radix notoginseng*, which is often used for ischemic heart disease. To investigate the possible protective effect of Rb1 against the damage of H9c2 cardiomyocytes that is induced by hypoxia–reoxygenation (H/R) and the

mechanisms underlying this protective effect, Label-Free Quantitative Proteomics was used. The results indicated that pretreatment with Rb1 caused an increase in cell viability compared with the H/R group. Moreover, pretreatment with Rb1 enhanced the capacity of cell antioxidants and inhibited cell apoptosis. Label-Free Quantification results revealed 29 differential proteins, including estrogen receptors α (ER α) and estrogen receptors β (ER β). Next, we used quantitative real-time PCR (qPCR) and western blotting analysis with specific kinase inhibitors to verify the proteomic results. In conclusion, Rb1 provided myocardial protection by inducing an estrogen receptor-dependent crosstalk among the Akt, JNK, and ERK1/2 pathways to prevent injury to H9c2 cardiomyocytes and apoptosis induced by H/R. The results might be highly important to the clinical efficacy of AMI treatment.

KEYWORDS:

Ginsenoside Rb1; H9c2 cardiomyocytes; Hypoxia-Reoxygenation; Oxidative Stress; Apoptosis; Label-Free Quantitative Proteomics

1. Introduction

Acute myocardial infarction (AMI) is the most common cause of disability and death worldwide¹. Current therapy for AMI involves reperfusion to the affected area via a thrombolytic therapy or angioplasty. However, ischemia/hypoxia followed by reperfusion induces further death of cardiomyocytes (myocardial ischemia-reperfusion injury [MIRI]), which involves an arrhythmia, an expansion of the infarct size and

persistent ventricular systolic dysfunction². MIRI is the primary reason for the poor prognosis of AMI³. Therefore, understanding the basis of reoxygenation and developing a cardioprotective drug that can alleviate MIRI could improve reoxygenation therapy when treating AMI.

Although the underlying mechanism of regulating MIRI is still poorly understood, oxidative stress is known to contribute to cell death⁴. Oxidative stress is a state of cellular redox imbalance in which the production of reactive oxygen species (ROS) overwhelms the endogenous antioxidant enzyme system. Excessive ROS damages the myocardia by triggering mitochondrial dysfunction and apoptosis⁵. Apoptosis is a process of programmed cell death that occurs in multicellular organisms, initiates shortly after the onset of myocardial infarction and becomes significantly enhanced during reperfusion⁶. Previous studies have shown that apoptosis serves an important function in AMI and MIRI processes^{7,8}. Therefore, antioxidant treatment is proposed to prevent oxidative stress-induced apoptosis. Antioxidant treatment can attenuate MIRI and improve cardiac function and has important clinical significance in AMI.

For many years, *Radix notoginseng* has been frequently used in the prevention and treatment of cardiovascular diseases in China, such as in the Guanxin Danshen Tablet, an herbal preparation. *P. notoginseng* saponins (PNS), including Ginsenosides Rg1, Rb1, Rh2, RK3, and Notoginsenoside R1, are generally believed to be the primary active ingredients that are responsible for the herbal drug's efficacy⁹⁻¹¹. Rb1 is the

primary active ingredient in PNS. Modern pharmacological research has demonstrated that Rb1 has many pharmacological activities, such as scavenging for free radicals¹², blocking calcium over-influx into the neurons¹³, inhibiting Na⁺ channel activity¹⁴, improving energy metabolism, and preserving the structural integrity of neurons¹⁵. Rb1 can protect against oxidative stress in dopaminergic cells and in ischemia–reperfusion^{16, 17}. Rb1 also has anti-hyperglycemic properties because it increases insulin sensitivity¹⁸, the survival of cultured neuronal cells after the excitotoxicity induced by kainic acid and glutamate¹⁹ and the neurite outgrowth of chick dorsal root ganglia²⁰. These beneficial effects of Rb1 are mediated by the scavenging of free radicals. Recent studies have demonstrated that Rb1 has estrogenic properties, as observed in human breast cancer MCF-7 cells^{21, 22}. Phytoestrogens are molecules of plant origin which are structurally and functionally similar to 17 β -estradiol²³. ER α and ER β are two distinct intracellular receptors that mediate the biological effects of estrogen, which are encoded by distinct genes with different expression levels in various tissues.

Recent research has demonstrated that Rb1 has protective effects on cerebral and myocardial ischemia injuries^{24, 25}. However, little is known concerning the mechanism behind the possible cardioprotective effect of Rb1. In this study, we used Label-Free Quantitative Proteomics to explore the mechanism underlying the cardioprotective effect of Rb1 in an *in vitro* model. Several widely used quantitative techniques of proteomic analysis include classical gel-based methods and LC (Liquid

chromatography)-based methods, such as isotopic labeling and relatively new Label-Free methods²⁶. However, classical gel-based methods, such as 2DE (Two dimensional electrophoresis) and DIGE (Difference gel electrophoresis), have disadvantages, such as low resolution of multiple proteins present in a single spot and difficulty in the identification of lowly expresses proteins, small proteins, and proteins at the extremes of the pI range²⁷. When using LC-based methods, such as ¹⁸O labeling, iTRAQ (isobaric tags for relative and absolute quantitation), SILAC (Stable isotope labeling with amino acids in cell culture), and ICAT (Isotope-coded affinity tag), the systematic identification and quantification of the detected proteins enables large-scale, relatively comprehensive global analyses²⁸⁻³¹. With increasing resolution and reproducibility from nano-HPLC systems combined with the improved mass accuracy and resolving power of mass spectrometers, thousands of proteins can be simultaneously identified and quantified. However, these methods also have drawbacks, including high cost, a high number of required samples, and complex experimental protocols; such drawbacks limit their application in studies²⁶.

Label-Free methods are LC-based methods that have recently been used as promising alternatives^{32,33}. Label-Free Quantitative approaches are rapidly becoming popular in the proteomics field for their rapid, straightforward, and low-cost measurements of protein expression levels in complex biological samples. The development of Label-Free methods was facilitated by crucial advances in the MS instrumentation, chromatography, and computation fields³⁴. Therefore, the use of Label-Free

Quantitative Proteomics to explore the underlying mechanisms of the cardioprotective effect of Rb1 is of considerable interest.

2. Materials and Methods

2.1. Materials

Ginsenoside Rb1 (molecular weight = 1109; purity > 98%; molecular structure shown in Fig. 1) was purchased from Shanghai Winherb Medical S&T Development (Shanghai, China). Rat embryonic cardiomyoblast-derived H9c2 cardiomyocytes were purchased from the Cell Bank of the Chinese Academy of Sciences (Shanghai, China). All of the cell culture materials were supplied from GIBCO (Grand Island, NY). 3-(4,5-Dimethylthiazol-2-yl)-2,5-diphenyltetrazolium bromide (MTT) and 5,5',6,6'-tetrachloro-1,1',3,3'-tetraethylbenzimidazolylcarbocyanine iodide (JC-1) were obtained from Enzo Life Sciences (PA, USA). The Annexin V/Propidium Iodide (PI) assay kit was purchased from Invitrogen (CA, USA). Caspase-3, -8, -9 Fluorometric Assay Kit, and the Terminal Deoxynucleotidyl Transferase Biotin-dUTP Nick End Labeling (TUNEL) Staining Kit were acquired from BioVision (CA, USA). The Image-iT™ LIVE Green Reactive Oxygen Species Detection Kit and Hoechst 33342 were acquired from Life Technologies (CA, USA). The kits for determining lactate dehydrogenase (LDH), superoxide dismutase (SOD), malondialdehyde (MDA), glutathione peroxidase (GSH-Px), catalase (CAT), and the Coomassie Protein Assay Kit were obtained from the Nanjing Jiancheng Institute of Biological Engineering (Nanjing, China). The Cell Nuclear Protein Extraction Kits, Mammalian

Protein Extraction Kits, Protease Inhibitor Cocktail, BCA Protein Assay Kit, Enhanced Chemiluminescence Western Blot Detection Kits, and RNAPure Tissue Kit were supplied by CWbiotech (Beijing, China). GoScripTM Reverse Transcription System was obtained from Promega (MA, USA). SYBR[®] Premix Ex TaqTM II (Tli RNaseH Plus) was supplied from TaKaRa (Japan). Specific kinase inhibitors, such as LY294002 (CID: 3973), were purchased from Calbiochem (CA, USA), whereas ICI-182780 (CID: 104741) was obtained from Sigma-Aldrich (MO, USA). All of the antibodies were obtained from Santa Cruz Biotechnology (Santa Cruz, CA), and other chemicals were obtained from Sigma (St. Louis, MO).

2.2. Cell culture and hypoxia-reoxygenation

H9c2 cardiomyocytes were cultured in high-glucose DMEM supplemented with 10% (v/v) fetal bovine serum and 1% penicillin/streptomycin (v/v). The cells were maintained at 37 °C with 100% relative humidity in a CO₂ incubator containing 5% CO₂. We switched the high-glucose DMEM medium with non-glucose DMEM to mimic ischemia. The H9c2 cells were incubated at 37 °C in an anaerobic glove box (Coy Laboratory, USA), in which normal air was removed by a pump and replaced with 5% H₂ and 95% N₂. After 6 h of hypoxia, we removed the cells out of the anaerobic glove box and replaced the medium with a high-glucose medium. The cells were maintained in a regular incubator to mimic reperfusion. The control cells were incubated under normal conditions with high-glucose DMEM.

2.3. Cell viability analysis

Cell viability was determined by a MTT assay. H9c2 cells were placed at a density of 1×10^5 cells/ml in 96-well plates and grown for 24 h. First, the cells underwent 6 h of hypoxia treatment, and cell viability was determined at 0, 3, 6, 9, 12, 18, and 24 h after reoxygenation to determine the optimal molding condition. Subsequently, 20 μ l of 5 mg/ml MTT solution was added to each well, and the cells were incubated for 4 h. The supernates were aspirated, and the formazan crystals in each well were dissolved in 150 μ l of dimethyl sulfoxide DMSO. Absorbance was measured at 570 nm on a microplate reader (Spectrafluor, TECAN, Sunrise, Austria). The optimal molding condition was identified; thereafter, the cells were incubated with different concentrations of Rb1 (3.125, 6.25, and 12.5 μ g/ml) for 24 h. We evaluated cell viability under normal conditions to determine whether Rb1 treatment could lead to cell proliferation and has a cytotoxic effect. The cells were then evaluated under optimal molding conditions to identify the optimal concentration.

2.4. Cytotoxicity analysis

The following four sets of experiments were performed: (1) control cells; (2) cells pretreated with Rb1 for 24 h; (3) H/R cells; and (4) H/R cells pretreated with Rb1 for 24 h. Cell death was evaluated using the LDH assay. H9c2 cardiomyocytes (3×10^5 cells/well) were fostered in 6-well plates. After treatment, we collected the medium to measure the LDH release using LDH assay kits following the manufacturer's instructions.

2.5. Detection of intracellular ROS production

The effect of Rb1 on intracellular ROS levels was measured using an Image-iT™ LIVE Green Reactive Oxygen Species Detection Kit according to manufacturer's instructions (CA, USA). First, we prepared a 10 mM carboxy-H₂DCFDA stock solution and a 25 μM carboxy-H₂DCFDA working solution. After treatment, the cells were harvested, placed into 5 ml round-bottom polystyrene tubes, and washed with phosphate-buffered saline (PBS) buffer. Subsequently, the cells were centrifuged for 5 min at 400 × g at room temperature, and the supernate was discarded. A sufficient amount of 25 μM carboxy-H₂DCFDA working solution was applied to cover the cells adhering to the coverslip(s). The mixture was incubated (protected from light) for 30 min at 37 °C. The cells were analyzed by flow cytometry (FACS Calibur™, BD Biosciences, CA, USA).

2.6. Determination of the levels of oxidative stress

H9c2 cardiomyocytes (3×10^5 cells/well) were seeded into poly-L-lysine-coated 6-well plates for 24 h. After treatment, the cells were harvested to determine the levels of SOD, MDA, GSH-Px and CAT (Nanjing Jiancheng Bioengineering Institute, China). Coomassie Protein Assay Kit was used to detect the cell protein concentration. We used the microplate reader (Spectrafluor, TECAN, Sunrise, Austria) to obtain the results.

2.7. Hoechst 33342 and PI double staining

Cells were double-stained with Hoechst 33342 and PI to quantitatively analyze apoptosis. H9c2 cardiomyocytes (1×10^5 cells/well) were fostered in 24-well plates for 24 h. After treatment, the cells were then washed twice with PBS and incubated with 10 $\mu\text{g/ml}$ Hoechst 33342 for 15 min at 37 °C in the dark. PI (100 $\mu\text{g/ml}$) was added (Invitrogen, CA, USA). Stained nuclei were immediately observed using fluorescence microscopy (Leica, Germany Q9). The results were analyzed using the Image-Pro Plus 6.0 software.

2.8. Flow cytometric detection of apoptosis

An Annexin V-FITC/PI apoptosis kit was used for the flow cytometry to measure the percentage of early apoptosis and necrosis according to the manufacturer's instructions (Invitrogen). After treatment, the cells were harvested, washed twice with cold PBS after treatment, and incubated with 5 μl of FITC-Annexin V and 1 μl of PI working solution (100 $\mu\text{g/ml}$) for 15 min in the dark at room temperature. Cellular fluorescence was measured by flow cytometry analysis with a flow cytometer (FACS Calibur™, BD Biosciences, CA, USA).

2.9. TUNEL staining

We used TUNEL to detect apoptosis. H9c2 cardiomyocytes (1×10^5 cells/well) were cultured in 24-well plates for 24 h. After treatment, H9c2 cardiomyocytes were fixed by incubating in a 10% neutral buffered formalin solution at room temperature for 30

min. H9c2 cardiomyocytes were incubated with a methanol solution containing 0.3% H₂O₂ for 30 min to stop the activity of endogenous peroxidase. H9c2 cardiomyocytes were treated with a permeabilizing solution (0.1% sodium citrate and 0.1% Triton X-100) at 4 °C for 2 min and were incubated in the TUNEL reaction mixture for 60 min at 37 °C. The morphological analysis was performed via fluorescence microscopy (Leica, Germany Q9). Four fields were randomly selected from each sample, and at least 100 cells were counted to calculate the rate of apoptosis. The results were analyzed using the Image-Pro Plus 6.0 software.

2.10. Caspase-3, -8, and -9 activity assay

Caspase-3, -8, and -9 activations were measured by Fluorescein Active Staining Kits (BioVision, CA, USA) according to the manufacturer's instructions. After treatment, almost 300 µl (1 × 10⁶ cells/ml) of the cells was incubated with 1 µl of substrate FITC-DEVD-FMK for 1 h at 37 °C and then centrifuged at 3000 rpm for 5 min. After removing the supernate and washing twice with cold PBS, the cells were re-suspended in 300 µl of wash buffer and were maintained on ice. Finally, the samples were analyzed by flow cytometry (FACS Calibur™, BD Biosciences, CA, USA) using the FL-1 channel.

2.11. Measurement of mitochondrial membrane potential

The change in mitochondrial membrane potential was detected by JC-1 staining. H9c2 cardiomyocytes (1 × 10⁵ cells/well) were cultured in 24-well plates. After treatment,

the cells were harvested and incubated with JC-1 (2 μ M final concentration) at 37 °C in the dark for 30 min. The cells were immediately observed using fluorescence microscopy (Leica, Germany Q9). The results were analyzed by the Image-Pro Plus 6.0 software.

2.12. Label-Free Quantitative Proteomics

H9c2 cardiomyocytes (3×10^5 cells/well) were seeded into poly-L-lysine-coated 6-well plates for 24 h. After treatment, the cell proteins were extracted using Mammalian Protein Extraction Kits (CWbiotech, Beijing, China). We measured the protein concentration using a BCA Protein Assay Kit (CWbiotech, Beijing, China) to ensure that the four sets of cells have equal amounts of protein. We placed 200 μ g of protein solution into a centrifuge tube. After centrifugation and reacted with trypsin at 37 °C overnight, this step was followed by a centrifugation at 12000 rpm for 20 min the next day to collect the peptide solution after digestion.

High pH reversed phase separation. The protease solution samples were dissolved using the mobile phase A, vortex oscillated, and centrifuged at 12000 rpm for 20 min, after which the supernatant was absorbed. Then, 100 samples (200 μ g) were loaded by an autosampler to the precolumn, and the gradient was eluted after desalination. The elution conditions were as follows: (1) From 0 min to 9 min, the proportion of the mobile phase was linear from 5% B to 15% B; (2) from 9 min to 30 min, the proportion of the mobile phase was linear from 15% B to 50% B; (3) from 30 min to

41 min, the proportion of the mobile phase was linear from 50% B to 90% B; (4) and 90% B was maintained for 19 min at a mobile phase flow rate of 230 $\mu\text{l}/\text{min}$. The eluted samples were collected for 27 copies, combined with the 15 copies according to the ultraviolet absorption of 214 nm, and dried.

For the LC-MS/MS analysis, the chromatographic column was a 2 cm, ID 100 μm , 5 μm , C18 EASY-column (Thermo Fisher, MA, USA). The precolumn was a 10 cm, ID 75 μm , 3 μm , C18 EASY-column (Thermo Fisher, MA, USA). Mass spectrometry was performed using a full scan (mass range, m/z 350–2000) Data Dependent MS/MS Scan, and 15 ions were sequentially selected by their ionic strength in a one-level mass spectrometry performed on the CID tandem mass spectrometry. The normalized collision energy was 35%, and the exclusion time was set to 30 s using the dynamic exclusion of tandem mass spectrometry^{35,36}.

The database analysis and Label-Free Quantification was determined using the following conditions³⁷: the retrieval software was Maxquant (version 1.2.2.5), the database was the Swiss-prot Human Proteome Database, the peptide error was 10 ppm, and the two-level error was 0.8 Da. The special digestion enzyme was trypsin, and the maximum allowable leakage cut was 2. The fixed modification involved carbamidomethylation (Cys) (+57.021 Da). The variable modification involved oxidation (Met) (+15.995 Da). A false discovery rate was controlled within 0.01, and the label-free quantification (LFQ) minimum ratio count was set to 2.

2.13. Quantitative Real-Time PCR (qPCR)

H9c2 cardiomyocytes (3×10^5 cells/well) were seeded into poly-L-lysine-coated 6-well plates for 24 h. After treatment, the total RNA was extracted using the RNApure Tissue Kit (CWbiotech, Beijing, China). The cDNA was synthesized from 2 μ g of total RNA using the GoScrip™ Reverse Transcription System (Promega, MA, USA). All qPCR processes were performed using the iQ5 Real-Time PCR Detection System (Bio-Rad, Hercules, CA, USA) and the Power SYBR Green PCR Master Mix (Applied Biosystems, Foster City, CA). β -Actin was detected as the internal control. The primers (Table 1) were acquired from NCBI Gene Bank and synthesized by Ruibiotech (Beijing, China).

2.14. Western blotting analysis

H9c2 cardiomyocytes (3×10^5 cells/well) were seeded into poly-L-lysine-coated 6-well plates for 24 h. After treatment, the whole proteins and the nuclear proteins of the cell were obtained using Mammalian and Nuclear Protein Extraction Kits with a Protease Inhibitor Cocktail (CWbiotech, Beijing, China). The protein concentration was determined using BCA Kits (CWbiotech, Beijing, China). Equal amounts of protein were separated by electrophoresis in 10% sodium dodecyl sulfate polyacrylamide gels and were transferred to nitrocellulose membranes. We incubated the membrane overnight at 4 °C with the following primary antibodies: Bcl-2 (N-19): sc-492; Bax (N-20): sc-493; Bad (H-168): sc-7869; Cytochrome-c (A-8): sc-13156;

Caspase-3 p11 (C-6): sc-271759; Caspase-8 p18 (D-8): sc-5263; Caspase-9 p10 (H-83): sc-7885; Bid (B-3): sc-373939; Bcl-x1 (H-5): sc-8392; PARP-1/2 (H-250): sc-7150; β -actin (C-2): sc-8432; ER α (H-184): sc-7207; ER β (Y-19): sc-6821; p-Akt1/2/3 (B-5): sc-271966; Akt1/2/3 (H-136): sc-8312; p-JNK (G-7): sc-6254; JNK (D-2): sc-7345; p-ERK 1/2 (12D4): sc-81492; ERK 1/2 (MK1): sc-135900; Nrf-2 (H-300): sc-13032; Lamin B (C-20): sc-6216; and HO-1 (H-105): sc-10789. The membranes were incubated at room temperature with their respective secondary antibodies for 3 h at a room temperature after washing with Tris-buffered saline and Tween 20 (TBST). The blots were developed using the Enhanced Chemiluminescence Western Blot Detection Kits (CWbiotech, Beijing, China) after rewashing with TBST and then were visualized using a molecular imager Lab software (BIO-RAD, USA). In specified experiments, the cells were pretreated with estrogen receptor inhibitor ICI-182780 (2 μ M) or PI3K/Akt inhibitor LY294002 (50 μ M) for 1 h, followed by incubation with Rb1 under H/R conditions. At least three independent experiments were performed to confirm the changes in protein levels.

2.15. Statistical analyses

All of the data were expressed as means \pm standard deviation (SD). Data were analyzed using the Student's t-test or one-way ANOVA followed by the Turkey's test or were analyzed using two-way ANOVA followed by the Bonferroni's multiple comparison test with Prism 5.00 software. Statistical significance was considered to be $P < 0.05$. All data were subjected to at least three separate experiments.

3. Results

3.1. Effect of H/R on cell viability and Ginsenoside Rb1 treatment inhibited H/R-induced cell death in H9c2 cardiomyocytes

To determine whether Rb1 could protect against cardiac injury induced by H/R *in vitro*, we first investigated the reoxygenation conditions leading to cell toxicity in H9c2 cardiomyocytes. After 6 h of hypoxia followed by reoxygenation treatment, cell viability was detected at 0, 3, 6, 9, 12, 18, and 24 h after reoxygenation by MTT assay. The cells in the control group were considered to be 100% viable. As shown in Fig. 2A, 6 h of hypoxia reduced approximately 14.79% of the cell viability, and reoxygenation led to a further time-dependent decline in cell viability. The reduced viability of cardiomyocytes was approximately 32.29% at 24 h after reoxygenation.

To identify the best dosage of Rb1 to protect against H/R-induced H9c2 cellular injury, we should evaluate the possibility that Rb1 may have a proliferation effect or be cytotoxic to H9c2 cardiomyocytes. After 24 h of treatment with various Rb1 concentrations (3.125, 6.25, and 12.5 $\mu\text{g/ml}$), no change in cell viability was detected by the MTT assay in H9c2 cardiomyocytes. Thus, our results excluded the possibility that Rb1 treatment changes the cellular viability (Fig. 2B).

After excluding the possibility of proliferation and cytotoxicity, we determined the best Rb1 dosage to protect against H/R-induced damage to H9c2 cardiomyocytes. We

treated H9c2 cardiomyocytes with various Rb1 concentrations (3.125, 6.25, and 12.5 $\mu\text{g/ml}$) for 24 h. The cells were exposed to 6 h of hypoxia followed by 24 h of reoxygenation. We identified the best dosage as 12.5 $\mu\text{g/ml}$ (Fig. 2C).

LDH leakage is a biomarker of cell death and was also detected. As shown in Fig. 2D, the following four sets of experiments were performed: (1) control cells; (2) cells pretreated with Rb1 (12.5 $\mu\text{g/ml}$) for 24 h; (3) H/R cells; and (4) H/R cells pretreated with Rb1 (12.5 $\mu\text{g/ml}$) for 24 h. H/R induced further release of LDH compared with the control group, and Rb1 significantly inhibited the release of LDH compared with the H/R group.

3.2. Ginsenoside Rb1-enhanced antioxidant capacity in H9c2 cardiomyocytes

ROS generation is among the common responses to cell damage and contributes to apoptotic progress³⁸. As shown in Fig. 3A, the H/R-induced group exhibited increased intracellular ROS levels compared with the control group, and Rb1 pretreatment significantly attenuated H/R-induced ROS release in H9c2 cells. Therefore, ROS generation was involved in the protection provided by Rb1 against H/R-induced cell injury.

H/R caused oxidative stress damage in H9c2 cells, as indicated by decreased SOD, CAT, and GSH-Px activities and increased lipid peroxidation (MDA production), but these changes were effectively alleviated by Rb1 (Fig. 3B-E).

3.3. Ginsenoside Rb1 treatment inhibited H/R-induced cell apoptosis in H9c2 cardiomyocytes

Apoptotic cell death was examined to investigate the type of cell death in H9c2 cardiomyocytes exposed to H/R and to gain insight into the mechanism underlying the myocardial protection of Rb1.

The morphological changes in apoptotic H9c2 cardiomyocytes induced by H/R were observed using Hoechst 33342/PI staining. Cells with blue nuclei were considered to be normal, whereas those with bright blue or red/pink nuclei were considered to be apoptotic. As shown in Fig. 4A, few cells with bright blue or red/pink nuclear staining were observed in the control group. H9c2 cells treated with H/R clearly exhibited staining, which indicated apoptosis. Pretreatment with Rb1 significantly alleviated the morphological changes triggered by H/R, as shown in Fig. 4C.

Phosphatidylserine externalization and DNA fragmentation are characteristic features of cells undergoing apoptosis. We used Annexin V/PI double staining and TUNEL to detect these features. H/R treatment remarkably augmented the proportion of Annexin V/PI-labeled cells (Fig. 4B) and the number of TUNEL-positive cells (Fig. 5A). The TUNEL-positive cell rate increased significantly compared with the rate in the control group (Fig. 5C), which suggested that H/R induced phosphatidylserine externalization and DNA fragmentation in H9c2 cardiomyocytes. Rb1 pretreatment effectively

reduced the proportion of cells that were apoptotic (Fig. 4D) as well as ameliorated the H/R-induced DNA fragmentation (Fig. 5C).

We also explored the intrinsic mitochondrial apoptotic pathway based on the depolarization of mitochondrial membrane and activation of caspase-3, -8, and -9 to confirm the characteristic features of apoptosis in H/R-treated H9c2 cardiomyocytes. A significant increase was observed in the percentage of cells that displayed a decreased mitochondrial membrane potential after the H/R treatment (Fig. 5B). This finding suggested that H/R depolarized the mitochondrial membrane of H9c2 cardiomyocytes. Rb1 pretreatment could increase the mitochondrial membrane potential (Fig. 5D). The activation of caspase-3, which results in the cleavage of PARP, is one of the key processes involved in apoptosis and contributes to myocardial dysfunction³⁹. Compared with H/R-treated H9c2 cardiomyocytes, myocardial caspase-3 activation was reduced in Rb1-pretreated cardiomyocytes (Fig. 6A). Apoptotic damage was activated in the H/R-treated H9c2 cardiomyocytes (Fig. 6B and Fig. 7), as shown by elevated caspase-8 and caspase-9 activities. Rb1 pretreatment ameliorated the apoptotic damage compared with the H/R-treated group.

3.4. Results and classification of H9c2 cardiomyocytes proteins identified by Label-Free Quantification

Proteomic analysis was performed on H9c2 cardiomyocytes. Equal amounts of proteins from H9c2 cardiomyocytes were loaded and separated in High performance

liquid chromatography. Differentially expressed proteins were identified and quantified by LFQ. The experiments were repeated thrice, and we identified approximately 6300 proteins in each group. The false-positive rate was approximately <1%. Based on LFQ intensity ratios (control / H/R > 2 and H/R / H/R+Rb1 < 0.5 or control / H/R < 0.5 and H/R / H/R+Rb1 > 2), 29 proteins, consisting of 14 downregulated and 15 upregulated proteins, were differentially expressed among the control, H/R, and H/R+Rb1 groups (Table 2). The differential proteins results in the three independent experiments are listed in the Supplementary Information. To understand the biological relevance of the identified proteins, Gene Ontology (GO) and UNIPROT were used to classify the differentially expressed proteins according to their molecular functions and biological processes (Supplementary Information Fig. 1). The proteins were classified into several significant groups of cellular components, biological processes, and molecular function⁴⁰.

The signal network of Rb1 was constructed, which was the protein–protein interaction network from estrogen receptor alpha (ER α) and estrogen receptor beta (ER β) to the possible signal-related proteins in the proteomic study (Supplementary Information Fig. 2). Data about protein–protein interactions from six publicly available databases, including Molecular Interaction database (MINT)⁴¹, IntAct⁴², Database of Interacting Proteins (DIP)⁴³ and biogrid⁴⁴, were integrated to construct the network.

3.5. Verification of differentially expressed proteins by qPCR

qPCR results showed that the mRNA expression levels of ER α and ER β were markedly reduced by H/R damage, and Rb1 significantly increased the level of expression in the pretreated group compared with the H/R group (Fig. 8A and Fig. 8B). The qPCR results are similar to the proteomic data.

3.6. Verification of differentially expressed proteins by western blotting analysis

To confirm the accuracy of protein identification by LFQ, ER α and ER β proteins were selected for validation by western blotting. The qPCR results showed that the protein expression levels of ER α and ER β were markedly reduced by H/R damage, and Rb1 significantly increased the level of expression in the pretreated group compared with the H/R group. Western blot analysis showed the same results as those of proteomics (Fig. 8). Western blotting results were analyzed by a Gel-Pro analyzer.

To elucidate the protective mechanism of Rb1, we examined the levels of apoptotic protein in H9c2 cardiomyocytes. The results showed that Rb1 can inhibit H/R-induced apoptosis (Fig. 9A). The Bcl-2 family including Bcl-2, Bax, Bad, Bid, and Bcl-xl plays an important role in H/R-induced apoptosis in various cells⁴⁵. Rb1 pretreatment can increase the Bcl-2/Bax ratio and the level of Bcl-xl expression (Fig. 9A), which were decreased by H/R damage (Fig. 9B and Fig. 9C), whereas the expression levels of Bad and Bid were increased by H/R damage (Fig. 9B and Fig. 9C). The caspase family also plays an important role in H/R-induced apoptosis in various cells⁴⁶. Cleaved caspase-3, -8, and caspase-9 expression levels were increased by H/R damage, but

Rb1 pretreatment could inhibit their expressions (Fig. 9B and Fig. 9C). PARP-1/2 shearing is an important index for caspase-3 activation. Rb1 pretreatment also inhibited the decrease in H/R-induced PARP-1/2 expression level (Fig. 9C). Cytochrome-c (cyt-c) release is the important index of apoptosis⁴⁷. H/R induced the release of cyt-c, whereas Rb1 pretreatment inhibited such release (Fig. 9B).

The direct interaction between ER α and PI3K defines a physiological, non-nuclear signaling pathway for estrogen action⁴⁸. Many studies have demonstrated that PI3K plays an important role in regulating the phosphorylation in Nrf2 and ARE-mediated phase II gene expression⁴⁹. To elucidate the protective mechanism of Rb1 further, we examined the activation of PI3K/Akt in H9c2 cardiomyocytes. The results (Fig. 8A and Fig. 10A) showed that the H/R damage decreased the expression of ER α , ER β , and p-Akt. Nuclear Nrf2 and HO-1 expressions slightly increased in the H/R group. Rb1 pretreatment resulted in higher expressions of ER α , ER β , p-Akt, nuclear Nrf2, and HO-1 than in the H/R group (Fig. 8D, Fig. 10B, and Fig. 10C). This finding suggested that Rb1 may be upregulated HO-1 via estrogen receptor-dependent activation of PI3K/Akt/Nrf2 pathways to induce protective effects. We also determined that H/R damage could increase the expressions of p-JNK and p-ERK 1/2, whereas Rb1 could decrease their expressions (Fig. 10B). Thus, we speculated the possibility of a crosstalk among the Akt, JNK, and ERK 1/2 pathways.

HO-1 is a rate-limiting enzyme with potent protective effects against oxidative stress.

H9c2 cardiomyocytes were pretreated with ICI-182780 (estrogen receptor inhibitor) or LY294002 (PI3K/Akt inhibitor) followed by Rb1 treatment to investigate whether Rb1 upregulated HO-1 via estrogen receptor-dependent activation of the PI3K/Akt pathways *in vitro*. Rb1 induced both ER α and ER β expressions and increased p-Akt levels (Fig. 11A). The Rb1-mediated increase in p-Akt expression was blocked by ICI 182780. By contrast, the Rb1-mediated augmentation of ER α and ER β expressions was not inhibited by LY294002. Thus, PI3K/Akt is the downstream regulator of ER α and ER β (Fig. 11B). Western blot analysis revealed that Rb1 potently increased the nuclear accumulation of Nrf2. The Rb1-mediated increase in nuclear accumulation of Nrf2 was abolished by ICI-182780 or LY294002 pretreatment (Fig. 11C). This finding suggested that Rb1 may activate Nrf2 via the estrogen receptor-dependent activation of the PI3K/Akt pathways. HO-1 expression was significantly increased in H9c2 cardiomyocytes treated with Rb1 alone but was reduced by pretreatment with ICI-182780 or LY294002 (Fig. 11A and Fig. 11C). The Rb1-induced reduction of expressions of p-JNK and p-ERK 1/2 could also be abolished by pretreatment with ICI-182780 or LY294002 (Fig. 11). This result further demonstrated the possibility of a crosstalk among the Akt, JNK, and ERK 1/2 pathways and suggested that JNK and ERK 1/2 are the downstream regulators of Akt.

4. Discussion

AMI remains a leading cause of death in epidemics worldwide, despite recent advancements in pharmacologic and early revascularization therapies. MIRI injury is a

major factor affecting the prevalence of AMI. Compared with reperfusion, reoxygenation causes further cardiomyocyte damage followed by hypoxia-induced changes⁵⁰. Much evidence has shown that apoptosis may be responsible for AMI and MIRI and may participate in post-infarction remodeling. Moreover, apoptosis is always an important research direction for therapeutic applications in AMI⁵¹.

Normally produced ROS can be scavenged by endogenous antioxidants, which are abundant in tissues. Protective enzymes can also scavenge endogenous ROS⁵². Heme Oxygenase-1 (HO-1) has received considerable attention among the various cytoprotective enzymes. HO-1 induction has been demonstrated to represent protective activity against brain oxidative injury⁵³ and is important in protecting against H/R injury in cardiomyocytes^{54,55}. HO-1 is a stress protein that can act against agents such as heme, endotoxins, and oxidants, which may induce oxidative injury⁵⁶. The transcriptional regulation of the HO-1 gene is related to the transcription factor, NF-E2-related factor 2 (Nrf2)⁵⁷. The function of Nrf2 is regulated by its dissociation from the cytoskeleton-associated protein Keap1, which acts as a cytoplasmic repressor of Nrf2. Nrf2 can translocate to the nucleus, where it interacts with other transcription factors when it dissociates from Keap1, binds to the antioxidant responsive element (ARE), and subsequently stimulates the expression of target genes⁵⁸. An increasing amount of evidence suggests that HO-1 can provide cytoprotection⁵⁹. Thus, the modulation of HO-1 expression may represent a novel target for therapeutic interventions, particularly the identification of a non-cytotoxic inducer of HO-1.

The principal finding of this study indicated that Rb1 prevents H/R-induced apoptosis in H9c2 cells via an estrogen receptor-dependent crosstalk among the Akt, JNK, and ERK 1/2 pathways. This study was the first to demonstrate the cardioprotective effects of Rb1 against H/R-induced oxidative stress and apoptosis in H9c2 cardiomyocytes. Rb1, a saponin of *P. notoginseng*, is structurally related to estradiol (Fig. 1) and exhibits a wide range of pharmacological effects, including antioxidant and anti-apoptotic properties^{60,61}. The model of H/R-induced oxidative damage to H9c2 cardiomyocytes is widely used to mimic oxidative stress⁶². In the present study, H/R-induced apoptosis in H9c2 cells showed significant increases in LDH release, DNA fragmentation, and apoptosis rates as well as a marked reduction in cell viability (Fig. 2-7). The MTT result of the H/R model showed a time-dependent decrease in cell viability from 0 h to 24 h of reoxygenation (Fig. 2A). This result suggested that cell viability decreased in H9c2 cardiomyocytes in response to hypoxia, as further evidenced by reoxygenation. Finally, we selected hypoxia 6 h and reoxygenation 24 h as the model. This model was used to explore the cardioprotective effects of Rb1. After observing the proliferation and cytotoxic effect of Rb1, we found that preconditioning with Rb1 at a concentration of 12.5 µg/ml for 24 h significantly enhanced the survival of H9c2 cardiomyocytes after H/R treatment (Fig. 2B and Fig. 2C). The protective effect of Rb1 pretreatment is manifested in an increase in cell viability and decrease in LDH leakage (Fig. 2D). An excessive amount of ROS damages various biomolecules via lipid peroxidation, protein oxidation, and DNA

damage, thereby resulting in mitochondrial dysfunction, caspase-3 activation, and cell apoptosis⁶³. In the present study, H/R-induced damage increased the intracellular ROS concentration in H9c2 cardiomyocytes (Fig. 3A), thereby increasing the levels of oxidative stress markers, such as lipid peroxidation products (MDA) (Fig. 3C). Rb1 preconditioning could also effectively increase the activities of SOD, GSH-Px, and CAT (Fig. 3B, Fig. 3D, and Fig. 3E). Rb1 pretreatment inhibited cellular apoptosis, as evidenced by the decrease in rates of apoptosis in the Hoechst 33342/PI double staining (Fig. 4A and Fig. 4C), Annexin V-FITC/PI detection (Fig. 4B and Fig. 4D), and TUNEL-positive cells (Fig. 5A and Fig. 5C). H/R treatment caused a remarkable loss in mitochondrial membrane potential (Fig. 5B and Fig. 5D) and an obvious increase in caspase-3 activation (Fig. 6A). However, Rb1 preconditioning effectively reversed the damages induced by H/R in H9c2 cardiomyocytes, thereby suggesting that Rb1 promoted the resistance of H9c2 cardiomyocytes to H/R-induced oxidative stress. Rb1 preconditioning could also effectively decrease the activation of caspase-8 and caspase-9 (Fig. 6B and Fig. 7). These results suggested that Rb1 inhibited H/R-induced apoptosis of H9c2 cardiomyocytes through antioxidation. However, the mechanism underlying such cardioprotective effects of Rb1 remains unclear.

Up to 29 proteins, including 14 downregulated and 15 upregulated proteins, were differentially expressed among the control, H/R and H/R+Rb1 groups by using Label-Free Quantitative Proteomic Analysis (Table 2). To understand the biological relevance of the identified proteins, GO and UNIPROT were used to classify the

differentially expressed proteins according to their molecular functions and biological processes (Supplementary Information Fig. 1). The signal work of Rb1 was also constructed (Supplementary Information Fig. 2). The protein expression levels of ER α and ER β significantly increased when comparing the H/R group to the H/R+Rb1 group. These findings may be attributed to the structure of Rb1, which is related to estradiol. Thus, ER α and ER β were selected as targets for investigation. The results of the Label-Free Quantitative Proteomics Analysis were verified and were the same as those of qPCR and western blotting (Fig. 8).

Western blot results showed that Rb1 pretreatment could inhibit the H/R-induced apoptosis in H9c2 cells (Fig. 9). Rb1 pretreatment could increase the Bcl-2/Bax ratio and Bcl-xl expression level, which were decreased by H/R damage (Fig. 9). Rb1 pretreatment could also decrease the levels of Bad and Bid expression, which were increased by H/R damage (Fig. 9B and Fig. 9C). The levels of cleaved caspase-3, -8, and -9 expression increased because of H/R damage, but Rb1 pretreatment inhibited this increase (Fig. 9B and Fig. 9C). PARP-1/2 shearing is an important index for caspase-3 activation. Rb1 pretreatment also inhibited the decrease in the level of PARP 1/2 expression induced by H/R (Fig. 9C). H/R induced the release of cyt-c, whereas Rb1 pretreatment inhibited this release (Fig. 9B).

The direct interaction between ER α and PI3K defines a physiological and non-nuclear signaling pathway for estrogen action⁴⁸. The phosphatidylinositol 3-kinase

(PI3K)/Akt and mitogen-activated protein kinase (MAPK) signaling pathways play important roles in controlling the survival and apoptosis of cardiomyocytes^{64, 65}. Several studies have demonstrated that the phosphorylation of Akt can activate Nrf-2, which regulates the expression of various antioxidant and phase II detoxification enzymes, such as HO-1. HO-1 is a subtype of heme oxygenase (HO) involved in cellular antioxidant defenses. Many reports have demonstrated that Akt phosphorylation-mediated upregulation of HO-1 can promote cell survival and protect against H/R injury in cardiomyocytes^{54, 55}. Considerable evidence has shown that MAPKs, including c-Jun NH2-terminal kinases (JNKs) and extracellular signal-regulated protein kinase (ERK1/2), play central roles in cell survival and apoptosis during IR injury⁶⁶. MAPK pathways, which are vital mediators of stress-induced apoptosis, have also been reported as mediators of Nrf2/Keap1/ARE signaling^{67, 68}. Given that both pro-apoptotic and anti-apoptotic effects of the JNK and ERK 1/2 pathways in apoptosis have been observed, their roles in apoptosis remain controversial depending on cell type and apoptotic stimuli⁶⁹⁻⁷¹.

Western blot results showed that the Rb1-pretreated group showed significantly increased protein levels of ER α , ER β , and p-Akt compared with the H/R group (Fig. 8D and Fig. 10B). Various studies have demonstrated that the activation of Akt could, in turn, activate Nrf2 and subsequently upregulate HO-1 expression^{55, 72}. After being released from Keap1 (the inhibitor of Nrf2), the activated Nrf2 translocates into the nucleus and accelerates HO-1 expression. HO-1 reportedly plays an important role in

protecting against I/R-induced injury⁷³. The protein levels of Nrf2 in nuclear extracts after H/R and HO-1 also significantly increased in the Rb1-pretreated group compared with the H/R group (Fig. 10A and Fig. 10C). In conclusion, Rb1 could prevent H/R-induced apoptosis of H9c2 cardiomyocytes via estrogen receptor-dependent PI3K/Akt/Nrf2/HO-1 signaling transduction pathways. We also found that Rb1 could markedly decrease the levels of p-JNK and p-ERK 1/2 expression compared with levels in the H/R group (Fig. 10B). Thus, we speculated that Rb1 could prevent H/R-induced apoptosis of H9c2 cells via an estrogen receptor-dependent crosstalk among the Akt, JNK, and ERK 1/2 pathways.

We used the specific kinase inhibitors ICI-182780 (estrogen receptor inhibitor) and LY294002 (PI3K/Akt inhibitor) to confirm our speculation. Western blot results showed that the increase in protein levels of ER α , ER β , p-Akt, Nuclear-Nrf2, and HO-1 in the group pretreated with Rb1 was eliminated by ICI-182780 and LY294002. However, the Rb1-mediated augmentation of ER α and ER β expressions was not inhibited by LY294002 (Fig. 11). This finding indicated that ER α and ER β existed in the upstream of PI3K/Akt and confirmed that Rb1 prevented H/R-induced apoptosis of H9c2 cardiomyocytes via estrogen receptor-dependent PI3K/Akt/Nrf2/HO-1 signaling transduction pathways. ICI-182780 and LY294002 could abolish the decrease in p-JNK and p-ERK 1/2 expression levels (Fig. 11). This result indicated that JNK and ERK 1/2 existed in the downstream of PI3K/Akt. In conclusion, Rb1 can prevent H/R-induced apoptosis of H9c2 cells via an estrogen receptor-dependent crosstalk

among the Akt, JNK, and ERK 1/2 pathways. Nevertheless, the precise mechanisms underlying such an effect require further investigation. Western blot results indicated that Rb1 inhibited the H/R-induced apoptosis of H9c2 cells through antioxidation. To our knowledge, this is the first report on the prevention of H/R-induced apoptosis in H9c2 cells by Ginsenoside Rb1 via an estrogen receptor-dependent crosstalk among the Akt, JNK, and ERK 1/2 pathways, as shown by the results of Label-Free Quantitative Proteomics Analysis.

This study is limited by the fact that the results were obtained from *in vitro* cell experiments. Thus, further verification using animal models is required. The protective effect of Rb1 should be confirmed in other apoptosis-related disease models to expand the clinically applied range of Rb1. The pharmacokinetic features of Rb1 in animals and humans should also be considered.

5. Conclusion

Rb1 provided cardioprotective effects against H/R-induced oxidative stress and apoptosis. A novel mechanism of Nrf2/ARE signaling activation, i.e., estrogen receptor-dependent crosstalk among Akt, JNK, and ERK 1/2 pathways, was responsible for the cardioprotective effect of Rb1 (Fig. 12). This finding may provide novel insights into the mechanism by which ginsenosides or phytoestrogens mediate Nrf2/ARE signaling activation and into the cardioprotective effects of *P. notoginseng*.

Supplementary Information

Refer to Web version on PubMed Central for supplementary information.

Acknowledgments

This work was partly supported by the National Natural Science Foundation of China (Grant no. 81374011), the Major Scientific and Technological Special Project for “Significant New Drugs Formulation” (Grant Nos. 2012ZX09501001004), and the Program for Innovative Research Team in IMPLAD (Grant no. IT1301).

References

1. G. Damiani, E. Salvatori, G. Silvestrini, I. Ivanova, L. Bojovic, L. Iodice and W. Ricciardi, *Clinical interventions in aging*, 2015, 10, 237-245.
2. D. J. Hausenloy and D. M. Yellon, *The Journal of clinical investigation*, 2013, 123, 92-100.
3. D. M. Yellon and D. J. Hausenloy, *The New England journal of medicine*, 2007, 357, 1121-1135.
4. Q. Zhao, X. Hu, L. Shao, G. Wu, J. Du and J. Xia, *Heart and vessels*, 2014, 29, 667-678.
5. X. Meng, G. Sun, J. Ye, H. Xu, H. Wang and X. Sun, *Free radical research*, 2014, 48, 445-460.
6. J. Gu, Y. Fan, X. Liu, L. Zhou, J. Cheng, R. Cai and S. Xue, *Cardiovascular research*, 2014, 104, 83-92.
7. Y. Sun, W. Yi, Y. Yuan, W. B. Lau, D. Yi, X. Wang, Y. Wang, H. Su, X. Wang, E. Gao, W. J. Koch and X. L. Ma, *Circulation*, 2013, 128, S113-120.
8. N. Wu, X. Zhang, P. Jia and D. Jia, *Biochemical and biophysical research communications*, 2015, DOI: 10.1016/j.bbrc.2015.01.084.
9. B. Sun, J. Xiao, X. B. Sun and Y. Wu, *British journal of pharmacology*, 2013, 168, 1758-1770.
10. D. Zhu, L. Wu, C. R. Li, X. W. Wang, Y. J. Ma, Z. Y. Zhong, H. B. Zhao, J. Cui, S. F. Xun, X. L. Huang, Z. Zhou and S. Q. Wang, *Journal of cellular biochemistry*, 2009, 108, 117-124.
11. H. Wang, P. Yu, H. Gou, J. Zhang, M. Zhu, Z. H. Wang, J. W. Tian, Y. T. Jiang and F. H. Fu, *Evidence-based complementary and alternative medicine : eCAM*, 2012, 2012, 506214.
12. D. Liu, H. Zhang, W. Gu, Y. Liu and M. Zhang, *PloS one*, 2013, 8, e79399.
13. M. Liu and J. Zhang, *Chinese medical journal*, 1995, 108, 544-547.
14. D. Liu, B. Li, Y. Liu, A. S. Attele, J. W. Kyle and C. S. Yuan, *European journal of pharmacology*, 2001, 413, 47-54.
15. K. Y. Jiang and Z. N. Qian, *Zhongguo yao li xue bao = Acta pharmacologica Sinica*, 1995, 16, 399-402.

16. Y. P. Hwang and H. G. Jeong, *Toxicology and applied pharmacology*, 2010, 242, 18-28.
17. Q. Sun, Q. T. Meng, Y. Jiang, H. M. Liu, S. Q. Lei, W. T. Su, W. N. Duan, Y. Wu, Z. Y. Xia and Z. Y. Xia, *PLoS one*, 2013, 8, e80859.
18. S. Park, I. S. Ahn, D. Y. Kwon, B. S. Ko and W. K. Jun, *Bioscience, biotechnology, and biochemistry*, 2008, 72, 2815-2823.
19. B. Liao, H. Newmark and R. Zhou, *Experimental neurology*, 2002, 173, 224-234.
20. N. Nishiyama, S. I. Cho, I. Kitagawa and H. Saito, *Biological & pharmaceutical bulletin*, 1994, 17, 509-513.
21. Y. J. Lee, Y. R. Jin, W. C. Lim, W. K. Park, J. Y. Cho, S. Jang and S. K. Lee, *Archives of pharmacological research*, 2003, 26, 58-63.
22. K. W. Leung, L. W. Cheung, Y. L. Pon, R. N. Wong, N. K. Mak, T. P. Fan, S. C. Au, J. Tombran-Tink and A. S. Wong, *British journal of pharmacology*, 2007, 152, 207-215.
23. R. J. Miksicek, *Proceedings of the Society for Experimental Biology and Medicine. Society for Experimental Biology and Medicine (New York, N.Y.)*, 1995, 208, 44-50.
24. X. S. Zeng, X. S. Zhou, F. C. Luo, J. J. Jia, L. Qi, Z. X. Yang, W. Zhang and J. Bai, *Canadian journal of physiology and pharmacology*, 2014, 92, 102-108.
25. S. Y. Zhan, Q. Shao, Z. Li, Y. Wang and X. H. Fan, *Zhongguo Zhong yao za zhi = Zhongguo zhongyao zazhi = China journal of Chinese materia medica*, 2014, 39, 1300-1305.
26. M. Bantscheff, S. Lemeer, M. M. Savitski and B. Kuster, *Analytical and bioanalytical chemistry*, 2012, 404, 939-965.
27. H. Issaq and T. Veenstra, *BioTechniques*, 2008, 44, 697-698, 700.
28. X. Yao, A. Freas, J. Ramirez, P. A. Demirev and C. Fenselau, *Analytical chemistry*, 2001, 73, 2836-2842.
29. P. L. Ross, Y. N. Huang, J. N. Marchese, B. Williamson, K. Parker, S. Hattan, N. Khainovski, S. Pillai, S. Dey, S. Daniels, S. Purkayastha, P. Juhasz, S. Martin, M. Bartlet-Jones, F. He, A. Jacobson and D. J. Pappin, *Molecular & cellular proteomics : MCP*, 2004, 3, 1154-1169.
30. S. E. Ong, B. Blagoev, I. Kratchmarova, D. B. Kristensen, H. Steen, A. Pandey and M. Mann, *Molecular & cellular proteomics : MCP*, 2002, 1, 376-386.
31. S. P. Gygi, B. Rist, S. A. Gerber, F. Turecek, M. H. Gelb and R. Aebersold, *Nature biotechnology*, 1999, 17, 994-999.
32. Z. Shen, P. Li, R. J. Ni, M. Ritchie, C. P. Yang, G. F. Liu, W. Ma, G. J. Liu, L. Ma, S. J. Li, Z. G. Wei, H. X. Wang and B. C. Wang, *Molecular & cellular proteomics : MCP*, 2009, 8, 2443-2460.
33. P. R. Cutillas and B. Vanhaesebroeck, *Molecular & cellular proteomics : MCP*, 2007, 6, 1560-1573.
34. W. Zhu, J. W. Smith and C. M. Huang, *Journal of biomedicine & biotechnology*, 2010, 2010, 840518.
35. J. R. Wisniewski, P. Ostasiewicz, K. Dus, D. F. Zielinska, F. Gnad and M. Mann, *Molecular systems biology*, 2012, 8, 611.
36. S. T. Tsai, C. C. Tsou, W. Y. Mao, W. C. Chang, H. Y. Han, W. L. Hsu, C. L. Li, C. N. Shen and C. H. Chen, *Proteome science*, 2012, 10, 69.
37. C. A. Lubber, J. Cox, H. Lauterbach, B. Fancke, M. Selbach, J. Tschopp, S. Akira, M. Wiegand, H. Hochrein, M. O'Keefe and M. Mann, *Immunity*, 2010, 32, 279-289.
38. K. Sinha, J. Das, P. B. Pal and P. C. Sil, *Archives of toxicology*, 2013, 87, 1157-1180.
39. X. Q. Li, W. Cao, T. Li, A. G. Zeng, L. L. Hao, X. N. Zhang and Q. B. Mei, *International*

- immunopharmacology*, 2009, 9, 1032-1041.
40. S. Briesemeister, T. Blum, S. Brady, Y. Lam, O. Kohlbacher and H. Shatkay, *Journal of proteome research*, 2009, 8, 5363-5366.
 41. L. Licata, L. Briganti, D. Peluso, L. Perfetto, M. Iannuccelli, E. Galeota, F. Sacco, A. Palma, A. P. Nardoza, E. Santonico, L. Castagnoli and G. Cesareni, *Nucleic acids research*, 2012, 40, D857-861.
 42. B. Aranda, P. Achuthan, Y. Alam-Faruque, I. Armean, A. Bridge, C. Derow, M. Feuermann, A. T. Ghanbarian, S. Kerrien, J. Khadake, J. Kerssemakers, C. Leroy, M. Menden, M. Michaut, L. Montecchi-Palazzi, S. N. Neuhauser, S. Orchard, V. Perreau, B. Roechert, K. van Eijk and H. Hermjakob, *Nucleic acids research*, 2010, 38, D525-531.
 43. L. Salwinski, C. S. Miller, A. J. Smith, F. K. Pettit, J. U. Bowie and D. Eisenberg, *Nucleic acids research*, 2004, 32, D449-451.
 44. B. J. Breitkreutz, C. Stark, T. Reguly, L. Boucher, A. Breitkreutz, M. Livstone, R. Oughtred, D. H. Lackner, J. Bahler, V. Wood, K. Dolinski and M. Tyers, *Nucleic acids research*, 2008, 36, D637-640.
 45. X. Peng, J. Shao, Y. Shen, Y. Zhou, Q. Cao, J. Hu, W. He, X. Yu, X. Liu, A. J. Marian and K. Hong, *Journal of molecular and cellular cardiology*, 2013, 59, 1-10.
 46. Z. B. Yang, B. Tan, T. B. Li, Z. Lou, J. L. Jiang, Y. J. Zhou, J. Yang, X. J. Luo and J. Peng, *Naunyn-Schmiedeberg's archives of pharmacology*, 2014, 387, 861-871.
 47. J. Sun, Y. Z. Li, Y. H. Ding, J. Wang, J. Geng, H. Yang, J. Ren, J. Y. Tang and J. Gao, *Brain research*, 2014, DOI: 10.1016/j.brainres.2014.09.039.
 48. T. Simoncini, A. Hafezi-Moghadam, D. P. Brazil, K. Ley, W. W. Chin and J. K. Liao, *Nature*, 2000, 407, 538-541.
 49. X. Yin, X. Wang, Z. Fan, C. Peng, Z. Ren, L. Huang, Z. Liu and K. Zhao, *Journal of cardiovascular pharmacology and therapeutics*, 2015, DOI: 10.1177/1074248414568196.
 50. A. L. Moens, M. J. Claeys, J. P. Timmermans and C. J. Vrints, *International journal of cardiology*, 2005, 100, 179-190.
 51. Y. Wang, H. Zhang, F. Chai, X. Liu and M. Berk, *BMC psychiatry*, 2014, 14, 349.
 52. X. L. Chen and C. Kunsch, *Current pharmaceutical design*, 2004, 10, 879-891.
 53. J. Chen, *Reviews in the neurosciences*, 2014, 25, 269-280.
 54. G. B. Sun, X. Sun, M. Wang, J. X. Ye, J. Y. Si, H. B. Xu, X. B. Meng, M. Qin, J. Sun, H. W. Wang and X. B. Sun, *Toxicology and applied pharmacology*, 2012, 265, 229-240.
 55. S. X. Liu, Y. Zhang, Y. F. Wang, X. C. Li, M. X. Xiang, C. Bian and P. Chen, *International journal of cardiology*, 2012, 160, 95-101.
 56. R. Foresti, M. Hoque, S. Bains, C. J. Green and R. Motterlini, *The Biochemical journal*, 2003, 372, 381-390.
 57. M. Zhao, H. Guo, J. Chen, J. Wang, H. Huang, S. Zheng, M. Hei, J. Li, S. Huang, J. Li, X. T. Ma, Y. Chen, L. Zhao, J. Zhuang and P. Zhu, *American journal of physiology. Cell physiology*, 2015, DOI: 10.1152/ajpcell.00369.2014, ajpcell.00369.02014.
 58. Y. Liu, J. Qiu, Z. Wang, W. You, L. Wu, C. Ji and G. Chen, *Journal of neurosurgery*, 2015, DOI: 10.3171/2014.11.jns132348, 1-9.
 59. S. Y. Hung, H. C. Liou, K. H. Kang, R. M. Wu, C. C. Wen and W. M. Fu, *Molecular pharmacology*, 2008, 74, 1564-1575.
 60. K. Radad, G. Gille, R. Moldzio, H. Saito and W. D. Rausch, *Brain research*, 2004, 1021, 41-53.

-
61. C. X. Yang, J. X. Liu, Z. L. Sun, X. Q. Gao, L. Deng and Q. L. Yuan, *Sichuan da xue xue bao. Yi xue ban = Journal of Sichuan University. Medical science edition*, 2008, 39, 214-217.
62. L. Sun, W. J. Zang, H. Wang, M. Zhao, X. J. Yu, X. He, Y. Miao and J. Zhou, *Cellular physiology and biochemistry : international journal of experimental cellular physiology, biochemistry, and pharmacology*, 2014, 34, 1614-1625.
63. Z. Radak, Z. Zhao, S. Goto and E. Koltai, *Molecular aspects of medicine*, 2011, 32, 305-315.
64. C. Deng, Z. Sun, G. Tong, W. Yi, L. Ma, B. Zhao, L. Cheng, J. Zhang, F. Cao and D. Yi, *PLoS one*, 2013, 8, e58371.
65. J. Chen, W. Wang, Q. Zhang, F. Li, T. Lei, D. Luo, H. Zhou and B. Yang, *PLoS one*, 2013, 8, e56224.
66. G. Vassalli, G. Milano and T. Moccetti, *Journal of transplantation*, 2012, 2012, 928954.
67. Z. Sun, Z. Huang and D. D. Zhang, *PLoS one*, 2009, 4, e6588.
68. X. Shi and B. Zhou, *Toxicological sciences : an official journal of the Society of Toxicology*, 2010, 115, 391-400.
69. S. W. Ryter, H. P. Kim, A. Hoetzel, J. W. Park, K. Nakahira, X. Wang and A. M. Choi, *Antioxidants & redox signaling*, 2007, 9, 49-89.
70. A. Das, F. N. Salloum, L. Xi, Y. J. Rao and R. C. Kukreja, *American journal of physiology. Heart and circulatory physiology*, 2009, 296, H1236-1243.
71. H. Y. Sun, N. P. Wang, M. Halkos, F. Kerendi, H. Kin, R. A. Guyton, J. Vinten-Johansen and Z. Q. Zhao, *Apoptosis : an international journal on programmed cell death*, 2006, 11, 1583-1593.
72. Y. M. Ha, M. Y. Kim, M. K. Park, Y. S. Lee, Y. M. Kim, H. J. Kim, J. H. Lee and K. C. Chang, *Apoptosis : an international journal on programmed cell death*, 2012, 17, 463-474.
73. B. Juhasz, B. Varga, A. Czompa, I. Bak, I. Lekli, R. Gesztelyi, J. Zsuga, A. Kemeny-Beke, M. Antal, L. Szendrei and A. Tosaki, *Journal of cellular and molecular medicine*, 2011, 15, 1973-1982.

Table.1. Primers used for qPCR analysis in this work.

Target genes	Primers	Primer sequences (5'-3')
ESR1	Forward	CCAGTCGAGCATCACTTACG
	Reverse	GGCTCGTTCTCCAGGTAGTA
ESR2	Forward	CTCACCGTCGAGCCTTAGTT
	Reverse	GCCGGGAACACTGTAGTTCA
Actin	Forward	GGTCGTACCACTGGCATTGT
	Reverse	GCTGTGGTGGTGAAGCTGTA

Table.2.Differentially expressed protein

UniProt	Accession number	Protein name	Gene name	Function	LFQ intensity ratio(Control / H/R)	P-Values	L
Q00566	IPI00829488	Methyl-CpG-binding protein 2	Mecp2	Transcription	2.09	0.0103	0
Q63190	IPI00551751	Emerin	Emd	Nuclear envelope	2.83	0.0146	0
A1A5P2	IPI00191512	Ribosome biogenesis regulatory protein homolog	Rrs1	Ribosome biogenesis	2.58	0.0338	0
P97570	IPI00189942	85/88 kDa calcium-independent phospholipase A2	Pla2g6	Lipid degradation	2.18	0.0197	0
Q4KM84	IPI00197166	Histidine protein methyltransferase 1 homolog	Mettl18	Methyltransferase	2.35	0.0001	0
Q05175	IPI00231651	Brain acid soluble protein 1	Basp1	Negative regulation of transcription	2.53	0.0044	0
P24051	IPI00210965	40S ribosomal protein S27-like	Rps27l	DNA repair	2.20	0.0169	0
P0CAX5	IPI00768467	Oligophrenin-1	Ophn1	Endocytosis	4.70	0.0144	0

P07335	IPI00470288	Creatine kinase B-type	Ckb	Brain development	5.47	0.0034	0
Q5PQS6	IPI00360893	Protein SMG9	Smg9	Nonsense-mediated mRNA decay	2.60	<0.0001	0
P05765	IPI00202725	40S ribosomal protein S21	Rps21	Endonucleolytic cleavage	2.28	0.0006	0
P19356	IPI00194345	Porphobilinogen deaminase	Hmbs	Heme biosynthesis	2.15	<0.0001	0
P06211	IPI00201392	Estrogen receptor	Esr1	Transcription	2.19	0.0006	0
Q62986	IPI00231871	Estrogen receptor beta	Esr2	Transcription	2.22	<0.0001	0
Q5U2P3	IPI00363605	AN1-type zinc finger protein 2A	Zfand2a	Zinc ion binding	0.17	0.0013	3
Q66HK4	IPI00851142	Transcription elongation factor B (SIII), polypeptide 3	Tceb3	Protein biosynthesis	0.33	0.0004	3
Q6P7B9	IPI00464460	Acyl-CoA desaturase 2	Scd2	Fatty acid biosynthesis	0.39	<0.0001	2
Q66H88	IPI00204594	Presqualene diphosphate phosphatase	Ppapdc2	Hydrolase	0.34	0.0006	2

Q62909	IPI00210128	Kinesin-like protein KIF2C	Kif2c	Cell cycle	0.49	0.0004	2
D3ZNS1	IPI00207827	Pleckstrin homology-like domain family B member 1	Phldb1	Unknown	0.46	<0.0001	2
Q5U305	IPI00363727	ER lumen protein-retaining receptor 2	Kdelr2	ER-Golgi transport	0.33	0.0002	2
P10818	IPI00194042	Cytochrome c oxidase subunit 6A1, mitochondrial	Cox6a1	Cytochrome-c oxidase activity	0.43	0.0212	3
G3V9Y2	Unknown	Lipid phosphate phosphohydrolase 1	Ppap2a	Lipid metabolic process	0.31	0.0029	2
Q68FY1	IPI00372778	Nucleoporin NUP53	Nup35	mRNA transport	0.39	0.0005	2
Q7TSE9	IPI00382352	HCLS1-associated protein X-1	Hax1	protein binding	0.41	0.0001	2
F1LPB5	Unknown	ER lumen protein retaining receptor	Kdelr3	protein retention in ER lumen	0.41	0.0208	4
Q8K4K5	IPI00325878	Lethal(2) giant larvae protein homolog 1	Llgl1	Exocytosis	0.26	0.0009	3

Q510H4	IPI00203757	Transmembrane and coiled-coil domains protein 1	Tmco1	Unknown	0.43	0.0112	3
M0RDM4	IPI00191077	Histone H2A	LOC680322	Nucleosome assembly	0.42	0.0002	2

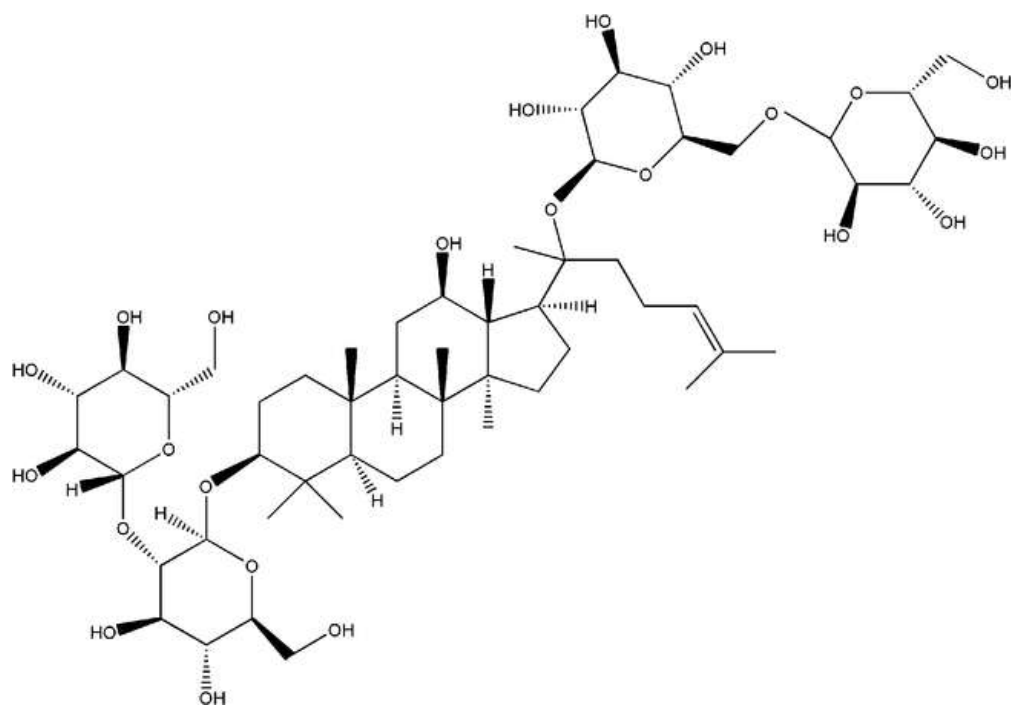


Fig. 1. Molecular structure of Ginsenoside Rb1.
55x38mm (300 x 300 DPI)

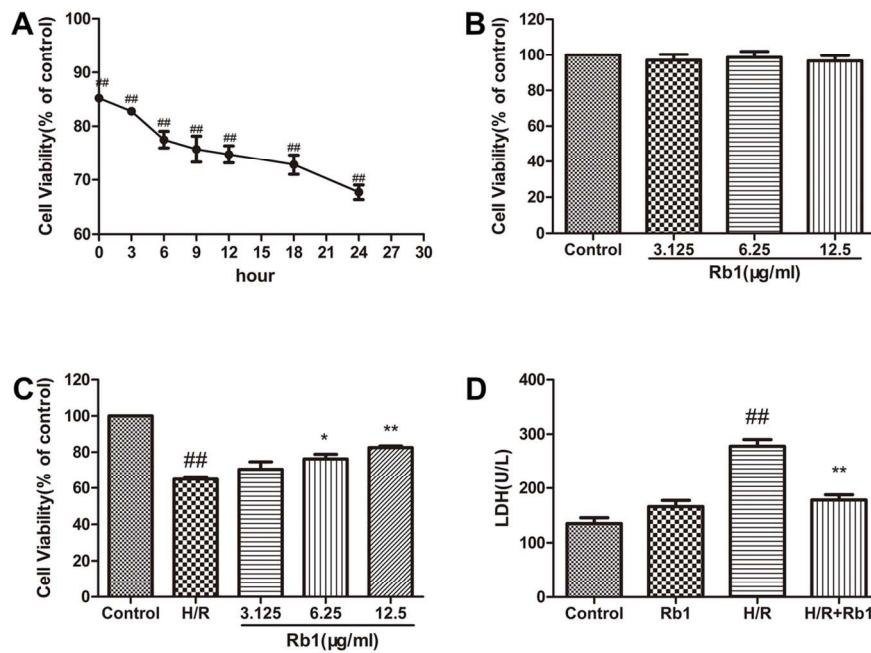


Fig. 2. The effects of H/R on cell viability and Ginsenoside Rb1 pretreatment inhibit H/R-induced cell death in H9c2 cells. (A) The effects of H/R on H9c2 cells. H9c2 cells were exposed to hypoxia for 6 h followed by reoxygenation for 24h. Cell viability was detected at 0, 3, 6, 9, 12, 18, and 24 h after reoxygenation using a MTT assay. (B) The cell viability was not significantly affected by Rb1 (3.125, 6.25, and 12.5 $\mu\text{g/ml}$) based on the results of the MTT assay. (C) H9c2 cells were pretreated with Rb1 (3.125, 6.25, and 12.5 $\mu\text{g/ml}$) for 24 h before H/R treatment. The cell viability was determined by a MTT assay. (D) The effect of Rb1 on LDH level in H9c2 cells was measured using an LDH assay kit. The results are represented as means \pm SD from three independent experiments. #P < 0.05 versus control; ##P < 0.01 versus control; *P < 0.05 versus H/R-treated cells; **P < 0.01 versus H/R-treated cells.

118x87mm (300 x 300 DPI)

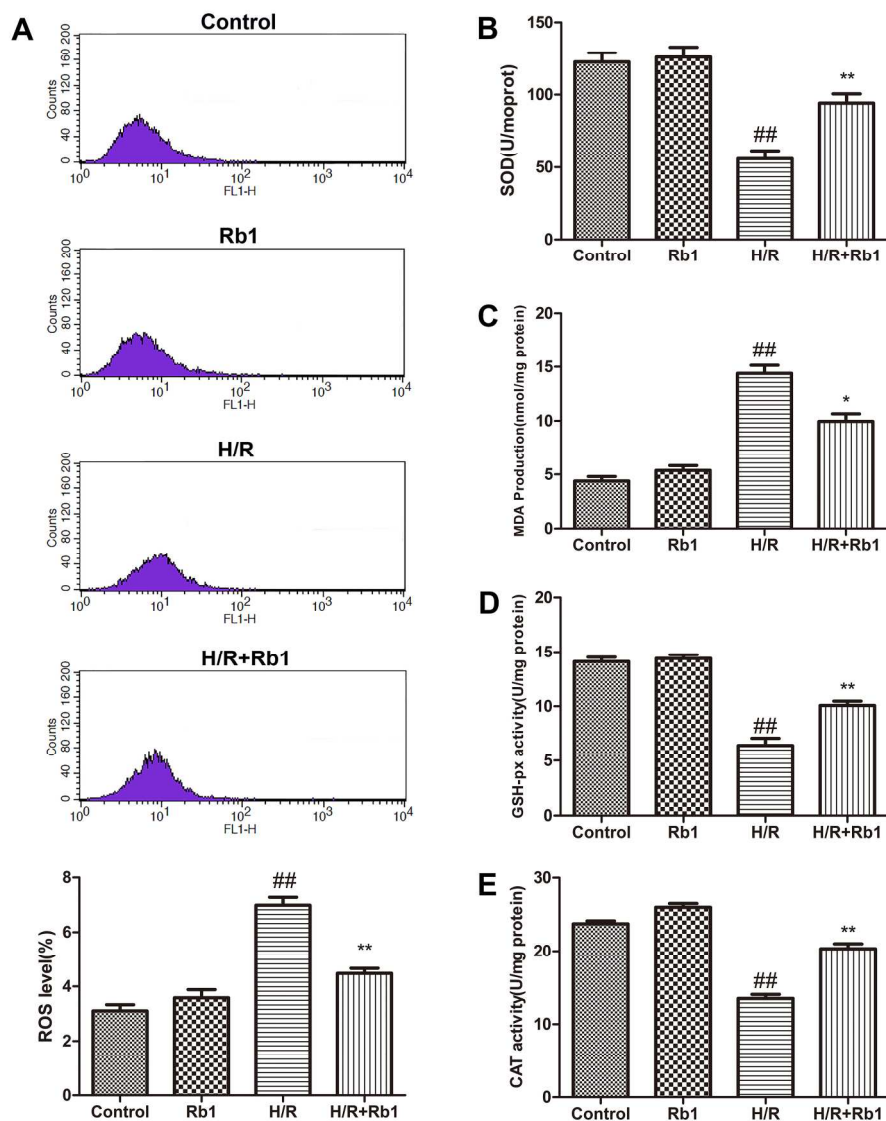


Fig. 3. The antioxidant capacity of Ginsenoside Rb1. H9c2 cells were exposed to hypoxia for 6 h followed by reoxygenation for 24h. (A) The intracellular ROS levels were measured using a flow cytometry assay. (B) The effects of Rb1 on the activities of SOD in H9c2 cardiomyocytes. (C) The effects of Rb1 on the activities of MDA in H9c2 cardiomyocytes. (D) The effects of Rb1 on the activities of GSH-Px in H9c2 cardiomyocytes. (E) The effects of Rb1 on the activities of CAT in H9c2 cardiomyocytes. The results are represented as means \pm SD from three independent experiments. #P < 0.05 versus control; ##P < 0.01 versus control; *P < 0.05 versus H/R-treated cells; **P < 0.01 versus H/R-treated cells.

194x236mm (300 x 300 DPI)

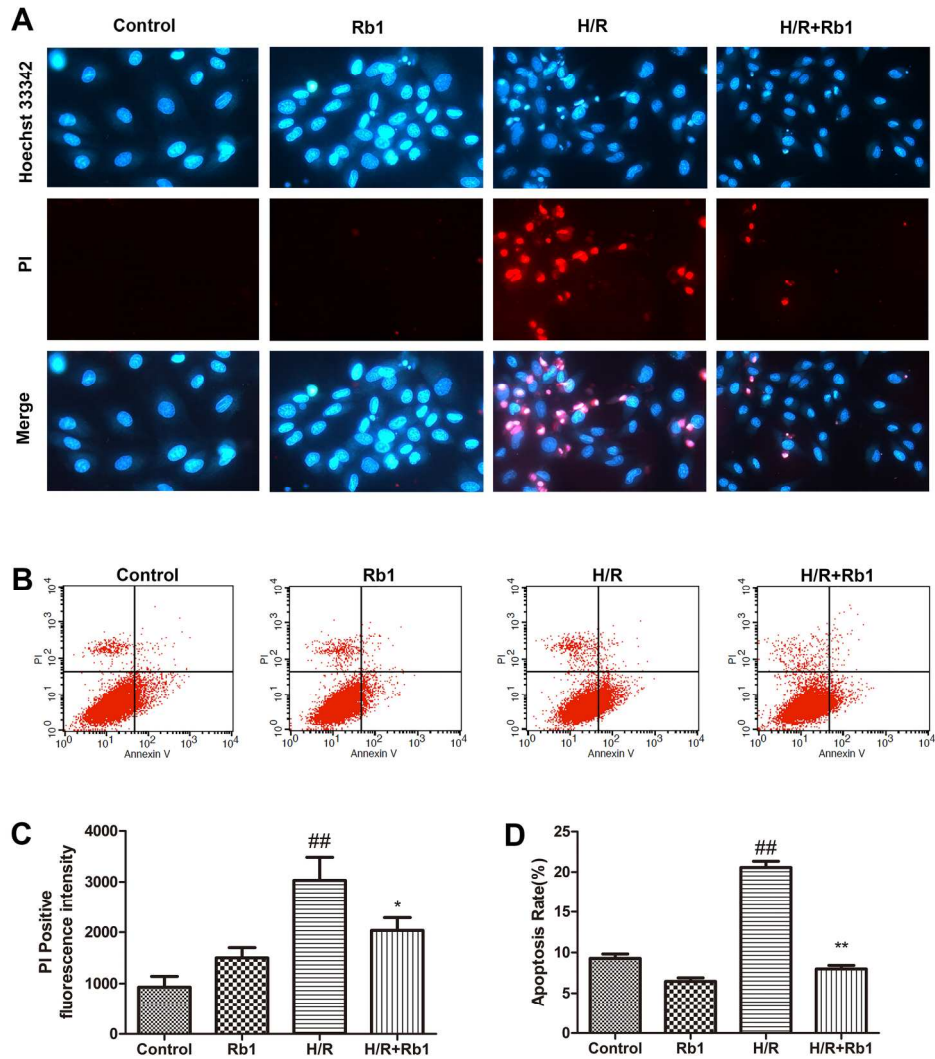


Fig. 4. The effects of H/R on cell apoptosis and Ginsenoside Rb1 pretreatment inhibit H/R-induced apoptosis in H9c2 cells. H9c2 cells were exposed to hypoxia for 6 h followed by reoxygenation for 24h. (A) Cell apoptosis and necrosis were assessed through Hoechst 33342/PI double staining by using fluorescence microscopy. (B) A scatter diagram of apoptotic H9c2 cells detected by Annexin V/PI double staining. (C) Quantitative analysis of PI-positive fluorescence intensity. (D) Quantitative analysis of apoptosis rate, as detected by Annexin V/PI double staining. The results are represented as means \pm SD from three independent experiments. [#] $P < 0.05$ versus control; ^{##} $P < 0.01$ versus control; ^{*} $P < 0.05$ versus H/R-treated cells; ^{**} $P < 0.01$ versus H/R-treated cells.

181x205mm (300 x 300 DPI)

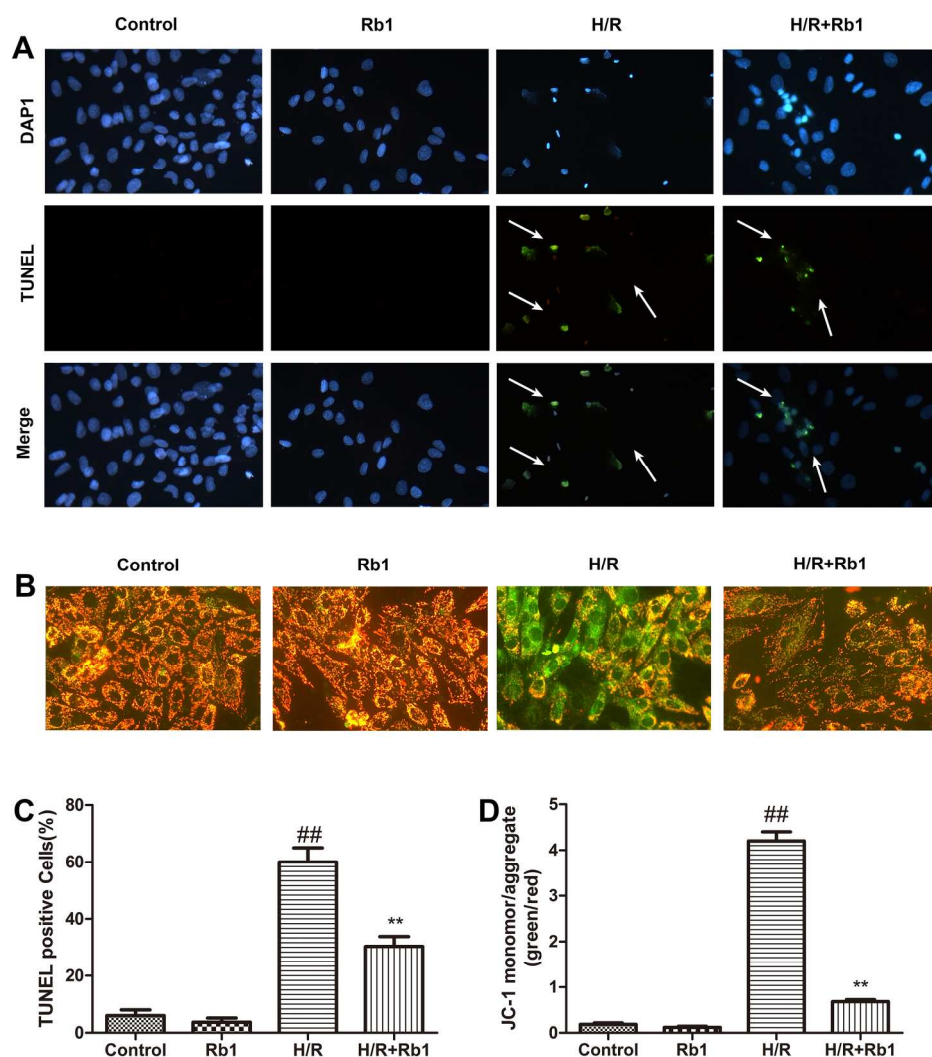


Fig. 5. Ginsenoside Rb1 attenuate H/R-induced DNA fragmentation and mitochondrial apoptotic cell death. H9c2 cells were exposed to hypoxia for 6 h followed by reoxygenation for 24h. (A) Fluorescence microscopy images of TUNEL staining. (B) Fluorescence microscopy images of JC-1 staining. (C) Quantitative analysis of TUNEL-positive cell rate. (D) Quantitative analysis of JC-1 monomer/aggregate rate. The results are represented as means \pm SD from three independent experiments. #P < 0.05 versus control; ##P < 0.01 versus control; *P < 0.05 versus H/R-treated cells; **P < 0.01 versus H/R-treated cells.

190x226mm (300 x 300 DPI)

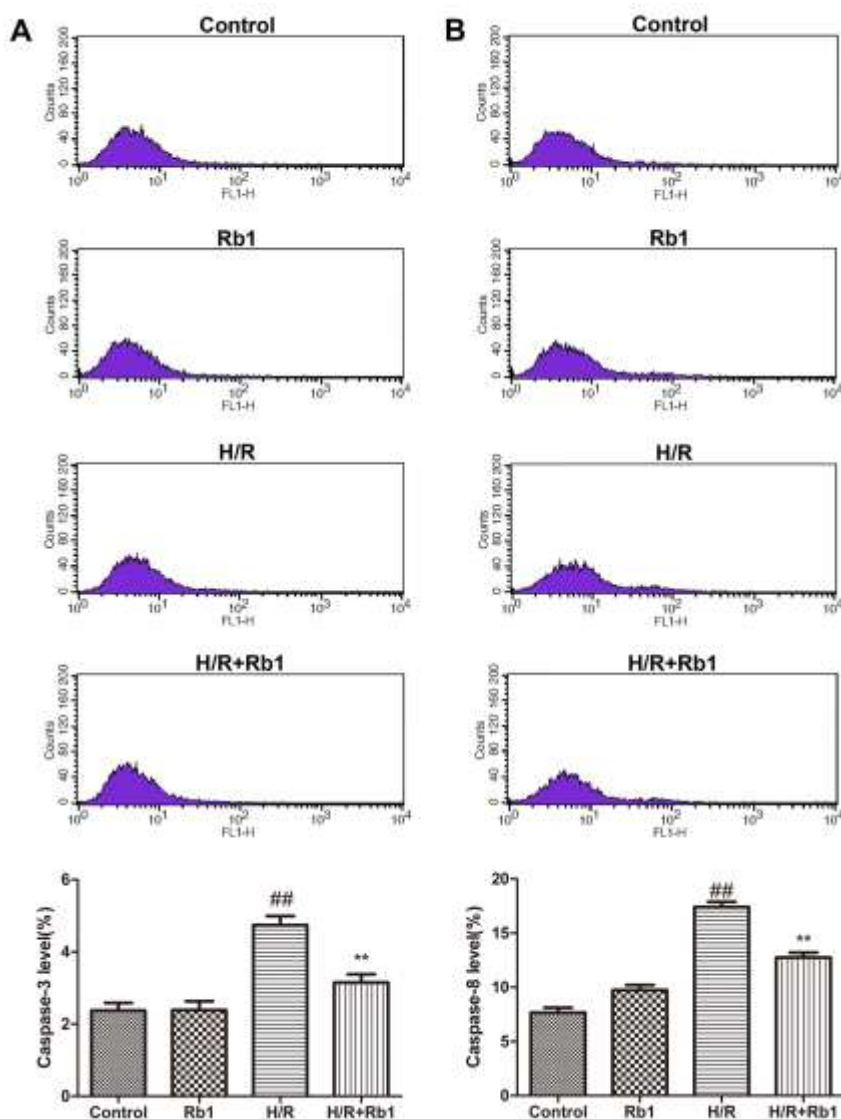


Fig. 6. The effects of Ginsenoside Rb1 on H/R-induced apoptosis in H9c2 cardiomyocytes. H9c2 cells were exposed to hypoxia for 6 h, followed by reoxygenation for 24h. (A) Rb1 attenuation of H/R-induced caspase-3 activity, as evaluated by flow cytometry. (B) Rb1 attenuation of H/R induced in caspase-8 activity, as evaluated by flow cytometry. The results are represented as means \pm SD from three independent experiments. #P < 0.05 versus control; ##P < 0.01 versus control; *P < 0.05 versus H/R-treated cells; **P < 0.01 versus H/R-treated cells.
194x236mm (300 x 300 DPI)

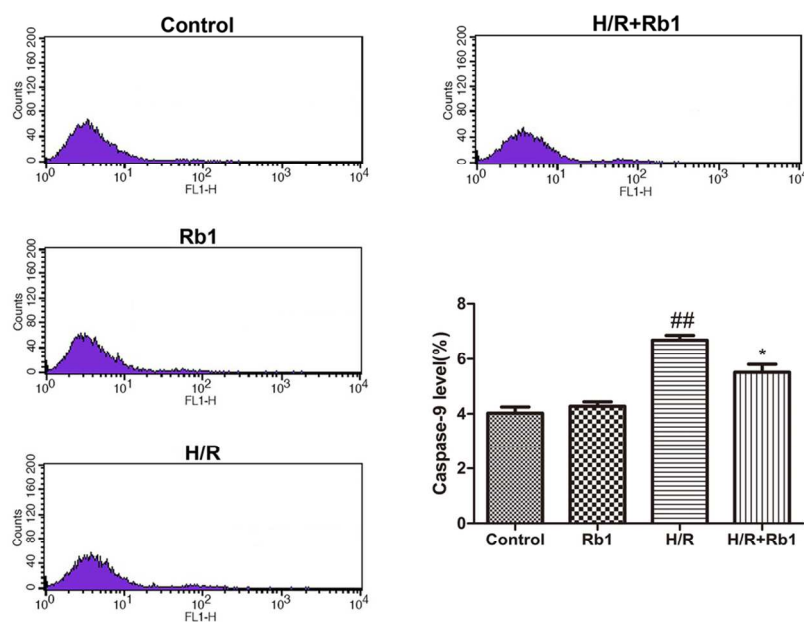


Fig. 7. The effects of Ginsenoside Rb1 on H/R-induced apoptosis in H9c2 cardiomyocytes. H9c2 cells were exposed to hypoxia for 6 h followed by reoxygenation for 24h. Rb1 attenuation of H/R-induced caspase-9 activity shown by flow cytometry. The results are represented as means \pm SD from three independent experiments. #P < 0.05 versus control; ##P < 0.01 versus control; *P < 0.05 versus H/R-treated cells; **P < 0.01 versus H/R-treated cells.
105x69mm (300 x 300 DPI)

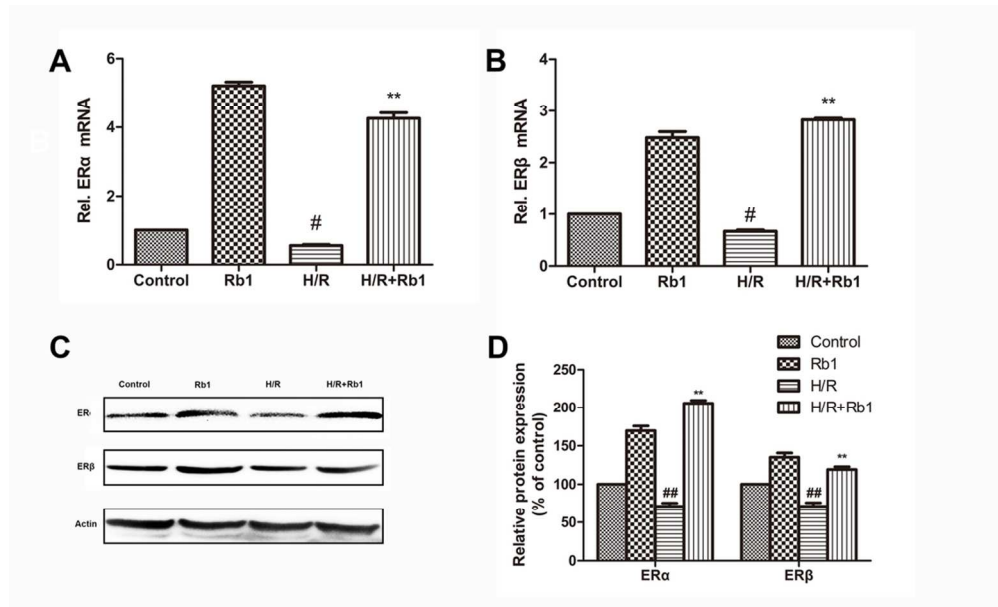


Fig. 8. Verification of Differentially Expressed Proteins by Quantitative real-time RT-PCR and western blotting. H9c2 cells were exposed to hypoxia for 6 h followed by reoxygenation for 24h. (A) The ER α expression in H9c2 cardiomyocytes was assayed by quantitative real-time RT-PCR. (B) The ER β expression in H9c2 cardiomyocytes was assayed by quantitative real-time RT-PCR. (C) Rb1 induced estrogen receptor. (D) The ER α and ER β expression in H9c2 cells was assayed by western blotting analysis using a Gel-Pro analyzer. The results are represented as means \pm SD from three independent experiments. #P < 0.05 versus control; ##P < 0.01 versus control; *P < 0.05 versus H/R-treated cells; **P < 0.01 versus H/R-treated cells.

96x58mm (300 x 300 DPI)

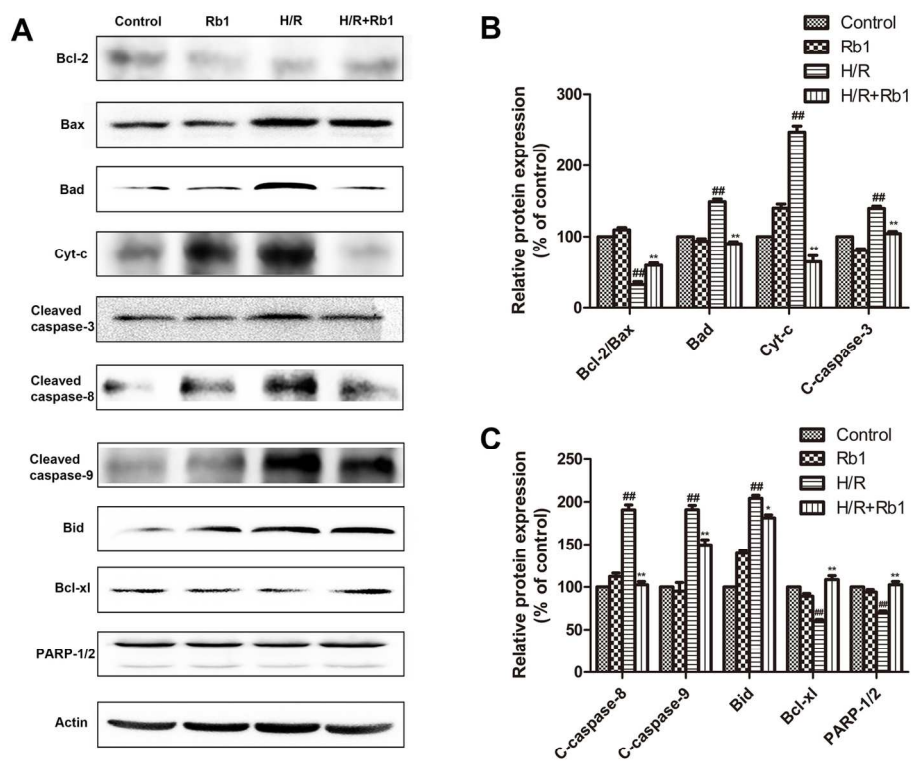


Fig. 9. The effects of H/R and Rb1 on apoptotic proteins. H9c2 cells were exposed to hypoxia for 6 h followed by reoxygenation for 24h. (A) The effects of H/R and Rb1 on Bcl-2 family and caspase protein family. (B) The Bcl-2/Bax expression ratio and Bad, cyt-c, cleaved caspase-3 expression in H9c2 cells was assayed by western blotting using a Gel-Pro analyzer. (C) The cleaved caspase-8, cleaved caspase-9, Bid, Bcl-xl, and PARP-1/2 expression in H9c2 cells was assayed by western blotting analysis using a Gel-Pro analyzer. The results are represented as means \pm SD from three independent experiments. #P < 0.05 versus control; ##P < 0.01 versus control; *P < 0.05 versus H/R-treated cells; **P < 0.01 versus H/R-treated cells.

143x129mm (300 x 300 DPI)

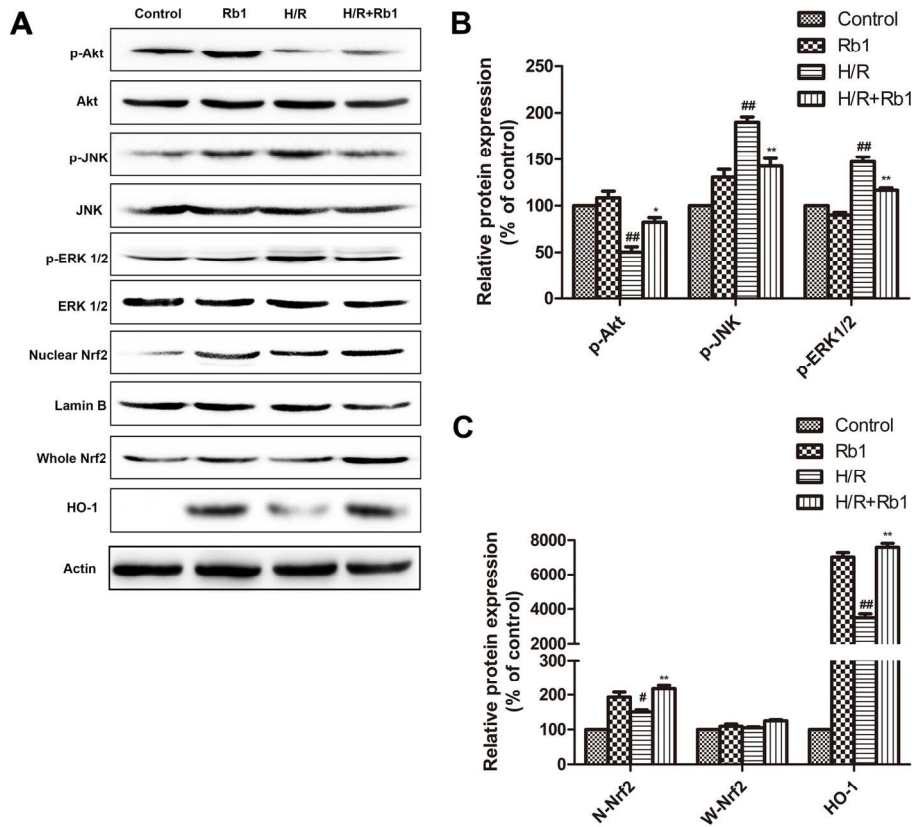


Fig. 10. The effects of H/R and Rb1 on PI3K/Akt, JNK, and ERK 1/2 pathways. H9c2 cells were exposed to hypoxia for 6 h followed by reoxygenation for 24h. (A) Rb1 induced an estrogen receptor-dependent crosstalk among the Akt, JNK, and ERK 1/2 pathways. (B) The p-Akt, p-JNK, and p-ERK 1/2 expression in H9c2 cells was assayed by western blotting using a Gel-Pro analyzer. (C) The nuclear Nrf2, whole Nrf2, and HO-1 expression in H9c2 cells was assayed by western blotting using a Gel-Pro analyzer. The results are represented as means \pm SD from three independent experiments. #P < 0.05 versus control; ##P < 0.01 versus control; *P < 0.05 versus H/R-treated cells; **P < 0.01 versus H/R-treated cells.

150x142mm (300 x 300 DPI)

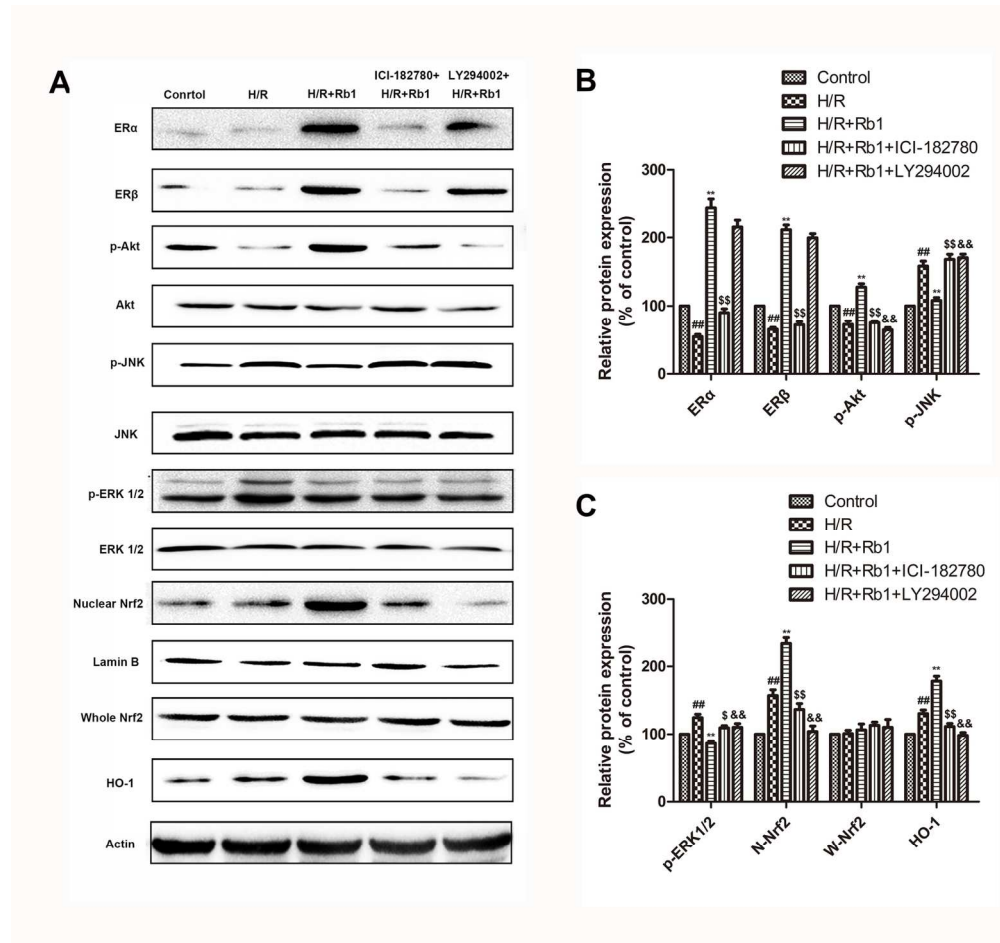


Fig. 11. Specific kinase inhibitors were used to confirm the effects of Rb1 on PI3K/Akt, JNK, and ERK 1/2 pathways. H9c2 cells were exposed to hypoxia for 6 h followed by reoxygenation for 24h. (A) Rb1 induced an estrogen receptor-dependent crosstalk among the Akt, JNK, and ERK 1/2 pathways by using specific kinase inhibitors. (B) The ER α , ER β , p-Akt, and p-JNK expression in H9c2 cells was assayed by western blotting using a Gel-Pro analyzer. (C) The p-ERK 1/2, nuclear Nrf2, whole Nrf2, and HO-1 expression in H9c2 cells was assayed by western blotting using a Gel-Pro analyzer. The results are represented as means \pm SD from three independent experiments. # $P < 0.05$ versus control; ## $P < 0.01$ versus control; * $P < 0.05$ versus H/R-treated cells; ** $P < 0.01$ versus H/R-treated cells; \$ $P < 0.05$ versus H/R-treated cells pretreated with Rb1; \$\$ $P < 0.01$ versus H/R-treated cells pretreated with Rb1; & $P < 0.05$ versus H/R-treated cells pretreated with Rb1; && $P < 0.01$ versus H/R-treated cells pretreated with Rb1.

151x142mm (300 x 300 DPI)

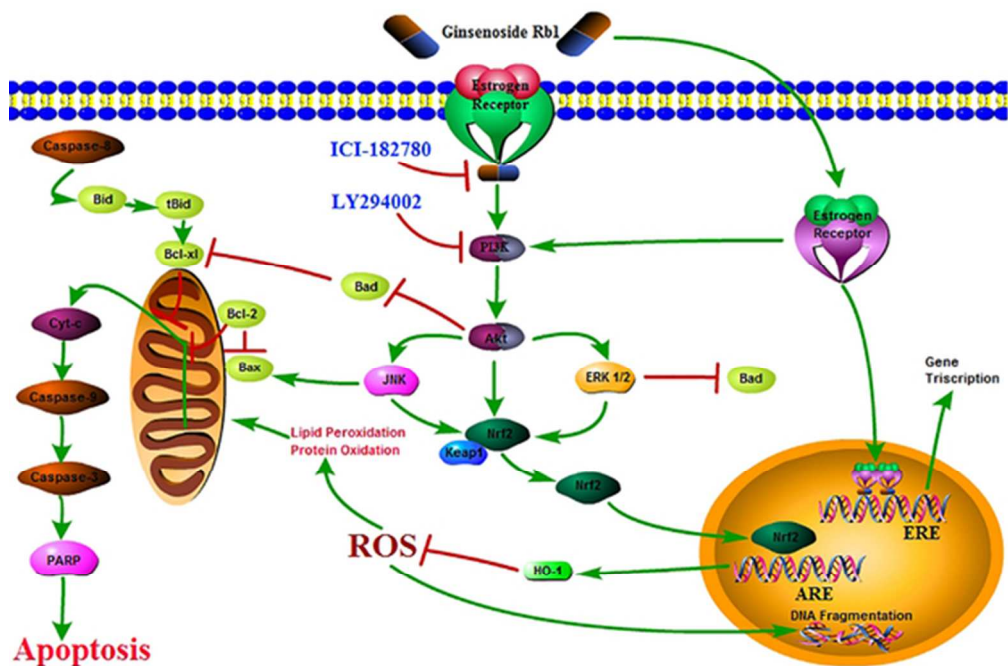


Fig. 12. Schematic of molecular mechanism responsible for cardioprotective effects of Rb1. Rb1 can prevent H/R-induced apoptosis of H9c2 cells via an estrogen receptor-dependent crosstalk among the Akt, JNK, and ERK 1/2 pathways.
52x37mm (300 x 300 DPI)